Chapter 6
Signal-to-Noise Ratio Estimation

Marvin K. Simon and Samuel Dolinar

Of the many measures that characterize the performance of a communication receiver, signal-to-noise ratio (SNR) is perhaps the most fundamental in that many of the other measures directly depend on its knowledge for their evaluation. In the design of receivers for autonomous operation, it is desirable that the estimation of SNR take place with as little known information as possible regarding other system parameters such as carrier phase and frequency, order of the modulation, data symbol stream, data format, etc. While the maximum-likelihood (ML) approach to the problem will result in the highest quality estimator, as is typically the case with this approach, it results in a structure that is quite complex unless the receiver is provided with some knowledge of the data symbols typically obtained from data estimates made at the receiver (which themselves depend on knowledge of the SNR). SNR estimators of this type have been referred to in the literature as *in-service* estimators, and the evaluation of their performance has been considered in [1]. Since our interest here is in SNR estimation for autonomous operation, the focus of our attention will be on estimators that perform their function without any data symbol knowledge and, despite their ad hoc nature, maintain a high level of quality and robustness with respect to other system parameter variations.

One such ad hoc SNR estimator that has received considerable attention in the past is the so-called *split-symbol moments estimator (SSME)* [2–5] that forms its SNR estimation statistic from the sum and difference of information extracted from the first and second halves of each received data symbol. Implicit in this estimation approach, as is also the case for the in-service estimators, is that the data rate and symbol timing are known or can be estimated. (Later on in the chapter we shall discuss how the SNR estimation procedure can be modified

when symbol timing is unknown.) In the initial investigations, the performance of the SSME was investigated only for binary phase-shift keying (BPSK) modulations with and without carrier frequency uncertainty and as such was based on real sample values of the channel output. In fact, it was stated in [1, p. 1683], in reference to the SSME, that "none of these methods is easily extended to higher orders of modulations." More recently, it has been shown [6] that such is not the case. Specifically, the traditional SSME structure, when extended to the complex symbol domain, is readily applicable to the class of M-phase-shift keying (M-PSK) ($M \geq 2$) modulations, and furthermore its performance is independent of the value of M! Even more generally, the complex symbol version of the SSME structure can also be used to provide SNR estimation for two-dimensional signal sets such as quadrature amplitude modulation (QAM) although the focus of the chapter will be on the M-PSK application.

We begin the chapter by defining the signal model and formation of the SSME estimator. Following this, we develop exact as well as highly accurate approximate expressions for its mean and variance for a variety of different scenarios related to the degree of knowledge assumed for the carrier frequency uncertainty and to what extent it is compensated for in obtaining the SNR estimate. With regard to the observables from which the SNR estimate was formed, two different models will be considered. In one case, we consider the availability of a plurality of uniformly spaced independent[1] samples of the received signal in each half-symbol, whereas in the second case only one sample of information from each half-symbol, e.g., the output of half-symbol matched filters, is assumed available—hence, two samples per symbol. Furthermore, we consider the wideband case wherein the symbol pulse shape is assumed to be rectangular, and thus the matched filters are in fact integrate-and-dump (I&D) filters. Finally, we discuss in detail a method for reconfiguring the conventional SSME to improve its performance for SNRs above a particular critical value. The reconfiguration, initially disclosed in [7], consists of partitioning the symbol interval into a larger (but even) number of subdivisions than the two that characterize the conventional SSME where the optimum number of subdivisions depends on the SNR region in which the true SNR lies. It will also be shown that these SNR regions can be significantly widened with very little loss in performance. Most important is the fact that, with this reconfiguration, the SNR estimator tracks the Cramer–Rao bound (with a fixed separation from it) on the variance of the estimator over the entire range of SNR values.

---

[1] Clearly the independence assumption on the samples is dependent on the sampling rate in relation to the bandwidth of the signal.

6.1 Signal Model and Formation of the Estimator

6.1.1 Sampled Version

A block diagram of the SSME structure in complex baseband form is illustrated in Fig. 6-1. Corresponding to the kth transmitted M-PSK symbol $d_k = e^{j\phi_k}$ in the interval $(k-1)\,T \le t \le kT$, the lth complex baseband received sample is given by[2]

$$y_{lk} = \frac{m}{N_s} d_k e^{j(\omega l T_s + \phi)} + n_{lk}, l = 0, 1, \cdots, N_s - 1, k = 1, 2, \cdots, N \qquad (6\text{-}1)$$

where ϕ and ω are the carrier phase and frequency uncertainties (offsets), N_s is the number of uniform samples per symbol and is assumed to be an even integer, $1/T_s$ is the sampling rate, N is the number of symbols in the observation, n_{lk} is a sample of a zero-mean additive white Gaussian noise (AWGN) process with variance σ^2/N_s in each (real and imaginary) part, and m reflects the signal amplitude. It is also convenient to denote the duration of a symbol by $T = N_s T_s$. Based on the above, the true symbol SNR is given by

$$R = \frac{m^2}{2\sigma^2} \qquad (6\text{-}2)$$

The received samples of Eq. (6-1) are first accumulated separately over the first and second halves of the kth symbol interval, resulting in the sums

$$Y_{\alpha_k} = \sum_{l=0}^{N_s/2-1} y_{lk} e^{-j\theta_{lk}} = \sum_{l=0}^{N_s/2-1} \left(\frac{m}{N_s} d_k e^{j([l/N_s]\delta + \phi)} + n_{lk} \right) e^{-j\theta_{lk}}$$

$$(6\text{-}3)$$

$$Y_{\beta_k} = \sum_{l=N_s/2}^{N_s-1} y_{lk} e^{-j\theta_{lk}} = \sum_{l=N_s/2}^{N_s-1} \left(\frac{m}{N_s} d_k e^{j([l/N_s]\delta + \phi)} + n_{lk} \right) e^{-j\theta_{lk}}$$

where $e^{-j\theta_{lk}}$ is a phase compensation that accounts for the possible adjustment of the lkth sample for phase variations across a given symbol due to the frequency offset and $\delta \triangleq \omega T$ is the normalized (to the symbol time) frequency offset. Next, the half-symbol sums in Eq. (6-3) are summed and differenced to produce

---

[2] For convenience, we assume that ϕ includes the accumulated phase due to the frequency offset up until the beginning of the kth symbol interval.
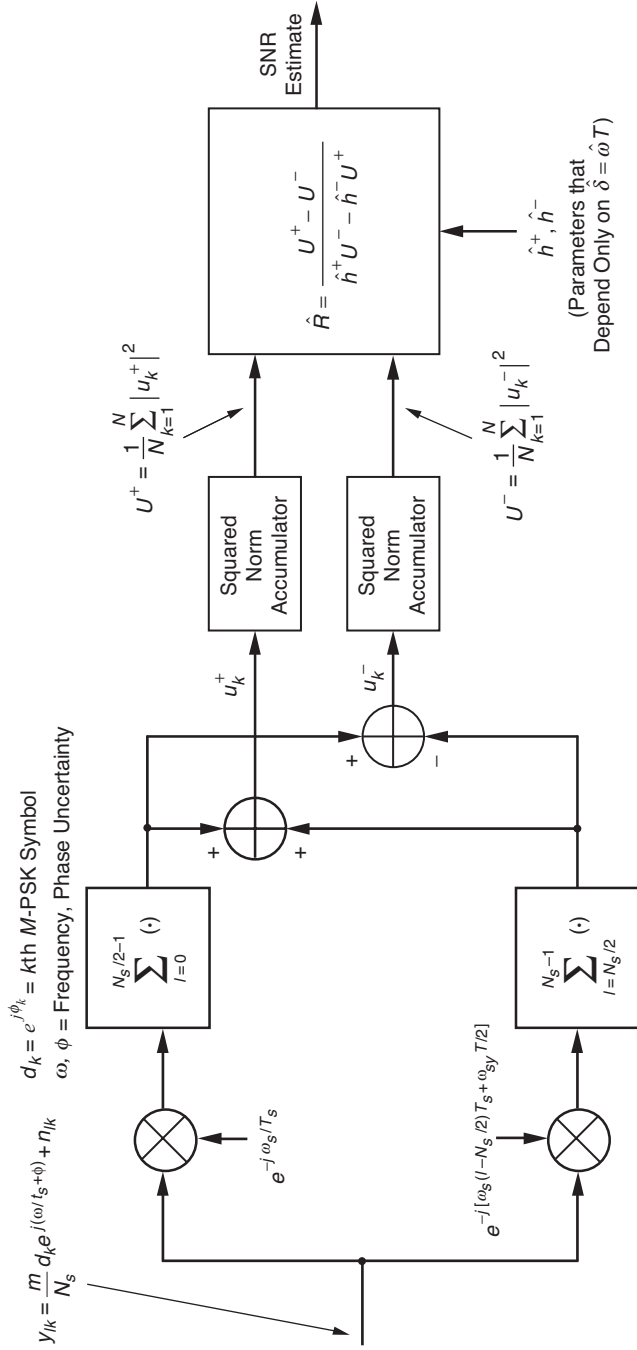
Fig. 6-1. Split-symbol SNR estimator for *M*-PSK modulation (sampled version).

$$u_k^{\pm} = Y_{\alpha_k} \pm Y_{\beta_k} \triangleq s_k^{\pm} + n_k^{\pm}, k = 1, 2, \cdots, N \tag{6-4}$$

where $s_k^{\pm}$ and $n_k^{\pm}$ respectively represent the signal and noise components of these half-symbol sums and differences and can be written in the form

$$s_k^{\pm} = \frac{m}{N_s} e^{j(\phi + \phi_k)} \left[\sum_{l=0}^{N_s/2-1} e^{j([l/N_s]\delta - \theta_{lk})} \pm \sum_{l=N_s/2}^{N_s-1} e^{j([l/N_s]\delta - \theta_{lk})} \right]$$

$$n_k^{\pm} = \sum_{l=0}^{N_s/2-1} n_{lk} e^{-j\theta_{lk}} \pm \sum_{l=N_s/2}^{N_s-1} n_{lk} e^{-j\theta_{lk}} \tag{6-5}$$

Finally, we average the squared norms of the half-symbol sums and differences over the N-symbol duration of the observation, producing

$$U^{\pm} = \frac{1}{N} \sum_{k=1}^{N} |u_k^{\pm}|^2 \tag{6-6}$$

Note that U^+ is a statistical measure of signal-plus-noise power where U^- is a statistical measure of noise power. Also, depending on the amount of information available for the frequency uncertainty ω and the method by which it is compensated for (if at all), the SNR estimator will take on a variety of forms (to be discussed shortly), all of which, however, will depend on the received complex samples only via the averages U^+ and U^-.

Making the key observation that the observables U^+ and U^- are independent random variables (RVs) and denoting the normalized squared norm of their sum and difference signal components by

$$h^{\pm} \triangleq \frac{|s_k^{\pm}|^2}{m^2} \tag{6-7}$$

then it is straightforward to show that their means and variances are given by

$$E\left\{U^{\pm}\right\} = 2\sigma^2 + |s_k^{\pm}|^2 = 2\sigma^2 \left(1 + h^{\pm}R\right)$$

$$\mathrm{var}\left\{U^{\pm}\right\} = \frac{4}{N}\sigma^2 \left(|s_k^{\pm}|^2 + \sigma^2\right) = \frac{4}{N}\sigma^4 \left(1 + 2h^{\pm}R\right) \tag{6-8}$$

Note that while the parameters $h^{\pm}$ depend on whether or not phase compensation is used and also on the frequency uncertainty, they are independent of the random carrier phase ϕ and the particular data symbol phase ϕ_k. As such, the $h^{\pm}$ are independent of the order M of the M-PSK modulation and, thus, so are the first and second moments of $U^{\pm}$ in Eq. (6-8).

Solving for the true SNR R from the first relation in Eq. (6-8) gives

$$R = \frac{E\{U^+\} - E\{U^-\}}{h^+ E\{U^-\} - h^- E\{U^+\}} \tag{6-9}$$

and the general form of the ad hoc SSME $\hat{R}$ is obtained by substituting the sample values $U^{\pm}$ for their expected values and the estimates $\hat{h}^{\pm}$ for their true values, namely,

$$\hat{R} = \frac{U^+ - U^-}{\hat{h}^+ U^- - \hat{h}^- U^+} \triangleq g\left(U^+, U^-\right) \tag{6-10}$$

For the case of real data symbols, i.e., BPSK, the estimator in Eq. (6-10) is exactly identical to the SSME considered in [2–5].

Note that in the absence of frequency uncertainty, i.e., $\delta = 0$, and thus of course no phase compensation, i.e., $\theta_{lk} = 0$, we have from Eq. (6-5) that $h^+ = 1$ and $h^- = 0$, in which case Eq. (6-9) simplifies to

$$R = \frac{E\{U^+\} - E\{U^-\}}{E\{U^-\}} \tag{6-11}$$

which appears reasonable in terms of the power interpretations of U^+ and U^- given above. Likewise, in this case we would have $\hat{h}^+ = 1$ and $\hat{h}^- = 0$, and the ad hoc SNR estimator would simplify to

$$\hat{R} = \frac{U^+ - U^-}{U^-} \tag{6-12}$$

6.1.2 I&D Version

A block diagram of the complex baseband SSME for this version is obtained from Fig. 6-1 by replacing the half-symbol accumulators by half-symbol I&Ds and is illustrated in Fig. 6-2. Corresponding to the kth transmitted M-PSK
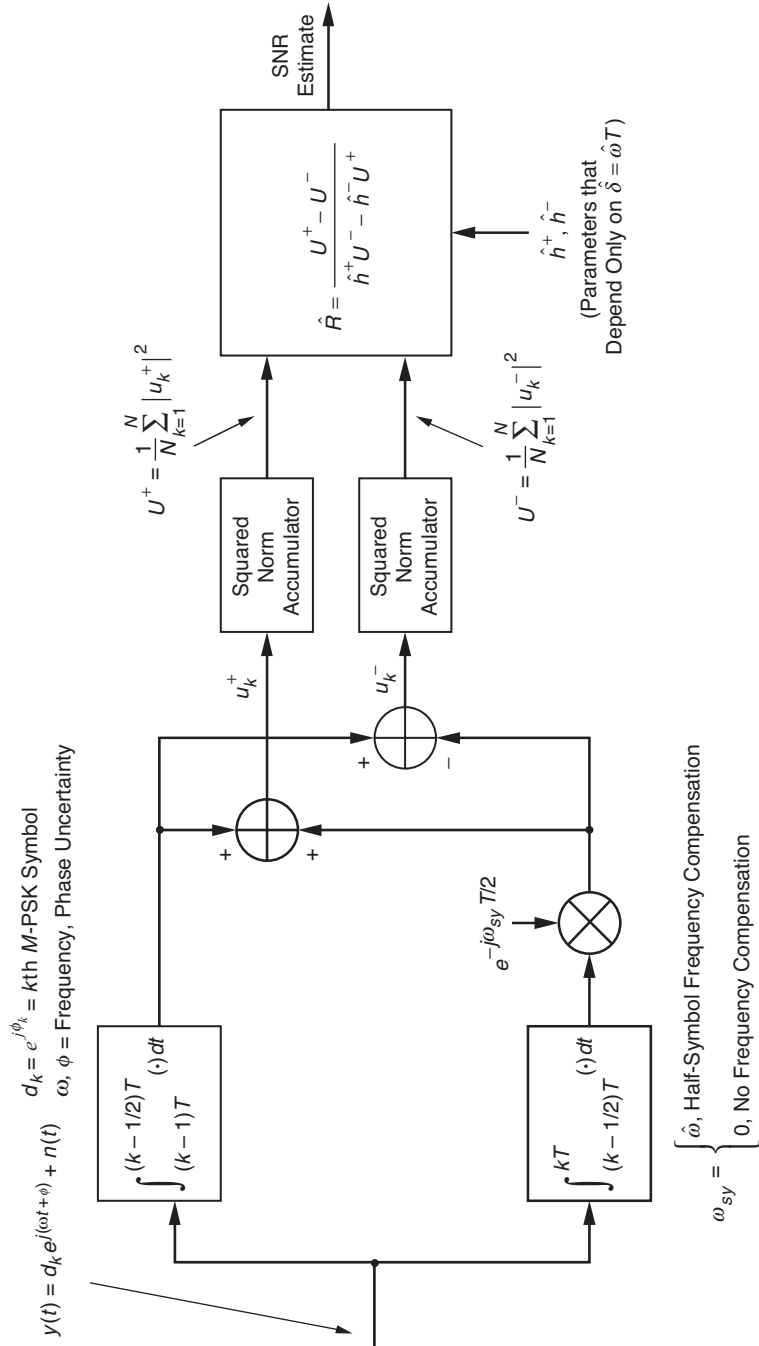
Fig. 6-2. Split-symbol SNR estimator for *M*-PSK modulation (I&D version).

symbol, the complex baseband received signal that is input to the first and second half-symbol I&Ds is given by

$$y(t) = md_k e^{j(\omega t + \phi)} + n(t), \quad (k-1)T \leq t < kT \tag{6-13}$$

where $n(t)$ is the zero-mean AWGN process. The outputs of these same I&Ds are given by

$$Y_{\alpha k} = md_k \frac{1}{T} \int_{(k-1)T}^{(k-1/2)T} e^{j(\omega t + \phi)} dt + \frac{1}{T} \int_{(k-1)T}^{(k-1/2)T} n(t) \, dt$$

$$= (md_k/2) \, e^{j\phi} e^{j\omega(k-3/4)T} \text{sinc} \, (\delta/4) + n_{\alpha k}$$

$$\tag{6-14}$$

$$Y_{\beta k} = \left(md_k \frac{1}{T} \int_{(k-1/2)T}^{kT} e^{j(\omega t + \phi)} dt + \frac{1}{T} \int_{(k-1/2)T}^{kT} n(t) \, dt \right) e^{-j\theta_k}$$

$$= \left((md_k/2) \, e^{j\phi} e^{j\omega(k-3/4)T} e^{j\omega T/2} \text{sinc} \, (\delta/4) + n_{\beta k} \right) e^{-j\theta_k}$$

where $\text{sinc} \, x \triangleq \sin x/x$, $n_{\alpha k}$, and $n_{\beta k}$ are complex Gaussian noise variables with zero mean and variance $\sigma^2/2$ for each real and imaginary component and $e^{-j\theta_k}$ is once again a phase compensation that accounts for the possible adjustment of the kth second-half sample for phase variations across a given symbol due to the frequency offset. As before, forming the half-symbol sums and differences produces

$$u_k^{\pm} = Y_{\alpha k} \pm Y_{\beta k} = (md_k/2) \, e^{j\phi} e^{j\omega(k-3/4)T} \text{sinc} \, (\delta/4) \left[1 \pm e^{j([\delta/2] - \theta_k)} \right]$$

$$+ n_{\alpha k} \pm n_{\beta k} e^{-j\theta_k} \triangleq s_k^{\pm} + n_k^{\pm} \tag{6-15}$$

If once again, as in Eq. (6-6), we average the squared norms of the half-symbol sums and differences over the N-symbol duration of the observation, then following the same series of steps as in Eqs. (6-7) through (6-9), we arrive at the ad hoc SNR estimator in Eq. (6-10).

6.2 Methods of Phase Compensation

For the sampled version of the SSME, we observe from Eq. (6-6) together with Eqs. (6-3) and (6-4) that the split-symbol observables $U^{\pm}$ are defined in terms of phase compensation factors $\left\{e^{-j\theta_{lk}}\right\}$ applied to the received samples $\{y_{lk}\}$ to compensate for phase variations across a given symbol due to the frequency offset ω. To perform this compensation, one requires some form of knowledge about this offset. In this regard, we shall assume that an estimate $\hat{\omega}$ of ω is externally provided. In principle, there are two ways in which this estimate can be used to provide the necessary compensation. The best-performing but most complex method adjusts the phases sample by sample, using a sample-by-sample compensation frequency $\omega_s = \hat{\omega}$. The alternative and less complex method does not compensate every sample but rather only once per symbol by adjusting the relative phase of the two half-symbols using a half-symbol compensation frequency $\omega_{sy} = \hat{\omega}$. Of course, the least complex form of phase compensation would be none at all even though the estimate $\hat{\omega}$ is available. In all three cases, the phase adjustment θ_{lk} can be written in the generic form

$$\theta_{lk} = \begin{cases} \omega_s l T_s, & 0 \leq l \leq N_s/2 - 1 \\ \omega_s \left(l - N_s/2\right) T_s + \omega_{sy} T/2, & N_s/2 \leq l \leq N_s - 1 \end{cases} \quad (6\text{-}16)$$

where

$$\omega_s = \omega_{sy} = \hat{\omega} \text{ for sample-by-sample phase compensation}$$

$$\omega_s = 0, \omega_{sy} = \hat{\omega} \text{ for half-symbol phase compensation} \quad (6\text{-}17)$$

$$\omega_s = \omega_{sy} = 0 \text{ for no phase compensation}$$

For the I&D version of the SSME, we only have the half-symbol phase compensation option available and thus $\theta_k = \omega_{sy} T/2 = \hat{\omega} T/2$. Of course, even though the estimate $\hat{\omega}$ is available, we again might still choose not to use it to compensate for the phase due to the frequency uncertainty. In this case, we would simply set $\theta_k = 0$ in Eqs. (6-14) and (6-15).

Besides being used for phase compensation of the samples or half-symbols that enter into the expressions for computing $U^{\pm}$, the frequency estimate also enters into play in determining the estimates $\hat{h}^{\pm}$ that are computed from $h^{\pm}$ by replacing ω with its estimate $\hat{\omega}$. Thus, the performance of the SSME will depend on the accuracy of the frequency estimate $\hat{\omega}$ with or without phase compensation. In the most general scenario, we shall consider a taxonomy of cases for analysis that, for the sampled version of the SSME, are illustrated by the tree diagram in Fig. 6-3. In this diagram, we start at the square node in the middle and proceed outward to any of the eight leaf nodes representing interesting com-

binations of $\omega, \hat{\omega}, \omega_{sy}$, and ω_s. The relative performance and complexity of each case is given qualitatively in Table 6-1, where the former is rated from worst (*) to best (****) and the latter from simplest (x) to most complex (xxxx). In the I&D version, a few of the tree branches of Fig. 6-3, namely, 2c and 3c, do not apply.
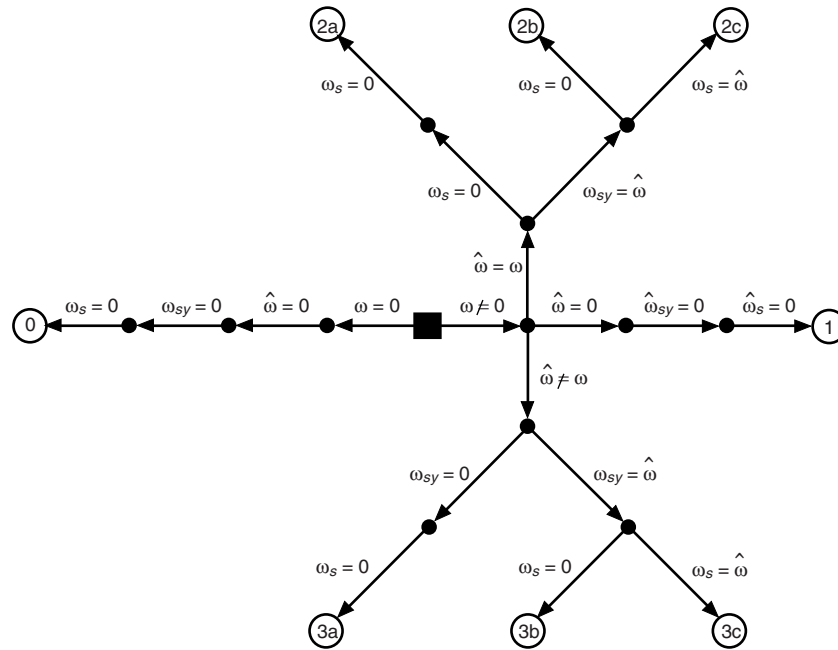

Fig. 6-3. A taxonomy of interesting cases for analysis.

**Table 6-1. Qualitative relative performance and complexity
of the various estimators.**

Case number	Frequency offset	Frequency estimate	Phase compensation	Performance	Complexity
0	0	Perfect	None	****	x
1	$\neq 0$	0	None	*	x
2a	$\neq 0$	Perfect	None	**	xx
2b	$\neq 0$	Perfect	Half-symbol	***	xxx
2c	$\neq 0$	Perfect	Sample-by-sample	****	xxxx
3a	$\neq 0$	Imperfect	None	* to **	xx
3b	$\neq 0$	Imperfect	Half-symbol	* to ***	xxx
3c	$\neq 0$	Imperfect	Sample-by-sample	* to ****	xxxx

6.3 Evaluation of $h^{\pm}$

For the sampled version SSME, we first insert the expression for the phase compensation in Eq. (6-16) into Eq. (6-5), which after simplification becomes

$$s_k^{\pm} = \frac{m}{N_s} e^{j(\phi + \phi_k)} \left(\frac{1 - e^{j(\delta - \omega_s T)/2}}{1 - e^{j(\delta - \omega_s T)/N_s}} \right) \left(1 \pm e^{j(\delta - \omega_{sy} T)/2} \right) \qquad (6\text{-}18)$$

Then taking the squared norm of Eq. (6-18) and normalizing by m^2 gives, in accordance with Eq. (6-7),

$$h^{\pm} = W_{N_s} (\delta_s) \frac{1 \pm W_0 (\delta_{sy})}{2} \qquad (6\text{-}19)$$

where

$$\delta_s = \delta - \omega_s T$$

$$\delta_{sy} = \delta - \omega_{sy} T \qquad (6\text{-}20)$$

and

$$W_0 (\delta) = \cos (\delta/2)$$

$$W_{N_s} (\delta) = \frac{\text{sinc}^2 (\delta/4)}{\text{sinc}^2 (\delta/2N_s)} \qquad (6\text{-}21)$$

are windowing functions. Note that $W_0 (\delta)$ has zeros at odd multiples of π, and $W_{N_s} (\delta)$ has zeros at all multiples of 4π except for multiples of $2N_s\pi$.

For the I&D version, $h^{\pm}$ is still given by Eq. (6-19) but with $W_{N_s} (\delta_s)$ replaced by

$$W (\delta) = \text{sinc}^2 (\delta/4) \qquad (6\text{-}22)$$

which is tantamount to taking the limit of $W_{N_s} (\delta)$ as N_s approaches infinity.

6.4 Mean and Variance of the SNR Estimator

In this section, we evaluate the mean and variance of $\hat{R}$ for a variety of special cases related to (1) the absence or presence of carrier frequency uncertainty ω and likewise for its estimation, (2) whether or not its estimate $\hat{\omega}$ is used for phase compensation, and (3) the degree to which $\hat{\omega}$ matches ω. In all cases involving frequency estimation, we treat $\hat{\omega}$ as a nonrandom parameter that is externally provided.

6.4.1 Exact Moment Evaluations

Since from Eq. (6-6) U^+ and U^- are sums of squared norms of complex Gaussian RVs, then they themselves are chi-square distributed, each with $2N$ degrees of freedom. Furthermore, since U^+ and U^- are independent, then the moments of their ratio can be computed from the product of the positive moments of U^+ and the positive moments of $1/U^-$ (or equivalently the negative moments of U^-), i.e.,

$$E\left\{\left(\frac{U^+}{U^-}\right)^k\right\} = E\left\{\left(U^+\right)^k\right\} E\left\{\left(U^-\right)^{-k}\right\} \tag{6-23}$$

Based on the availability of closed-form expressions for these positive and negative moments for both central and non-central chi-square RVs [8], we shall see shortly that it is possible to make use of these expressions to evaluate the first two moments of the SSME either in closed form or as an infinite series whose terms are expressible in terms of tabulated functions. In each case considered, the method for doing so will be indicated but the explicit details for carrying it out will be omitted for the sake of brevity, and only the final results will be presented.

●**Case 0: No Frequency Uncertainty**
$\left(\omega = \hat{\omega} = \omega_{sy} = 0 \Rightarrow \delta = \hat{\delta} = \delta_{sy} = \hat{\delta}_{sy} = 0\right)$

Since in this case $W(0) = W_{N_s}(0) = W_0(0) = 1$, then we have from Eq. (6-19) that $h^+ = \hat{h}^+ = 1, h^- = \hat{h}^- = 0$ and $\hat{R} = (U^+ - U^-)/U^-$, which was previously arrived at in Eq. (6-12). Since $\hat{R} + 1 = U^+/U^-$ is the ratio of a non-central to a central chi-square RV, each with $2N$ degrees of freedom, then the mean and variance of $\hat{R}$ can be readily evaluated as

$$E\left\{\hat{R}\right\} = \frac{N}{N-1}R + \frac{1}{N-1}$$

$$\text{var}\left\{\hat{R}\right\} = \frac{1}{N-2}\left(\frac{N}{N-1}\right)^2\left[(1+2R)\left(\frac{2N-1}{N}\right) + R^2\right]$$

(6-24)

Since N is known, the bias of the estimator is easily removed in this case by defining a *bias-removed estimator* $\hat{R}_0 = [(N-1)/N]R - 1/N$ whose mean and variance now become

$$E\left\{\hat{R}_0\right\} = R$$

$$\text{var}\left\{\hat{R}_0\right\} = \frac{1}{N-2}\left[(1+2R)\left(\frac{2N-1}{N}\right) + R^2\right]$$

(6-25)

•**Case 1: Frequency Uncertainty, No Frequency Estimation (and thus No Phase Compensation)**
$\left(\omega \neq 0, \hat{\omega} = \omega_{sy} = \omega_s = 0 \Rightarrow \delta \neq 0, \hat{\delta} = 0, \delta_{sy} = \delta_s = \delta, \hat{\delta}_{sy} = \hat{\delta}_s = 0\right)$

For this case, $h^\pm = W_{N_s}(\delta)[1 \pm W_0(\delta)]/2$ for the sampled version or $h^\pm = W(\delta)[1 \pm W_0(\delta)]/2$ for the I&D version, $\hat{h}^+ = 1, \hat{h}^- = 0$, and again $\hat{R} = (U^+ - U^-)/U^-$. Since h^- is non-zero, then $\hat{R} + 1 = U^+/U^-$ is now the ratio of two non-central chi-square RVs, each with $2N$ degrees of freedom. Using [8, Eq. (2.47)] to evaluate the first and second positive moments of U^+ and the first and second negative moments of U^-, then using these in Eq. (6-23) allows one, after some degree of effort and manipulation, to obtain the mean and variance of $\hat{R} + 1$, from which the mean and variance of $\hat{R}$ can be evaluated as

$$E\left\{\hat{R}\right\} = \frac{N}{N-1}(1+h^+R)_1F_1\left(1; N; -Nh^-R\right) - 1$$

$$\text{var}\left\{\hat{R}\right\} = \left(\frac{N}{N-1}\right)^2\left\{\left(\frac{N-1}{N-2}\right)\left[\frac{(1+2h^+R)}{N} + \left(1+h^+R\right)^2\right]\right.$$

(6-26)

$$\left. \times\ _1F_1\left(2; N; -Nh^-R\right) - \left(1+h^+R\right)^2\left[_1F_1\left(1; N; -Nh^-R\right)\right]^2\right\}$$

where $_1F_1(a; b; z)$ is the confluent hypergeometric function [9]. Since ω and thus $h^{\pm}$ are now unknown, the bias of the estimator cannot be removed in this case. Furthermore, since $_1F_1(a; b; 0) = 1$, then when $h^+ = 1$ and $h^- = 0$, Eq. (6-26) immediately reduces to Eq. (6-24) as it should.

•Case 2a: Frequency Uncertainty, Perfect Frequency Estimation, No Phase Compensation

$$\left(\omega \neq 0, \hat{\omega} = \omega, \omega_{sy} = \omega_s = 0 \Rightarrow \delta = \hat{\delta} \neq 0, \delta_{sy} = \hat{\delta}_{sy} = \delta_s = \hat{\delta}_s = \delta\right)$$

For this case, $h^{\pm} = \hat{h}^{\pm} = W_{N_s}(\delta)[1 \pm W_0(\delta)]/2$ for the sampled version or $h^{\pm} = \hat{h}^{\pm} = W(\delta)[1 \pm W_0(\delta)]/2$ for the I&D version, and $\hat{R}$ is given by the generic form of Eq. (6-10). Obtaining an exact compact closed-form expression in this case is much more difficult since $h^{\pm}$ and $\hat{h}^{\pm}$ are now *all* non-zero. However, it is nevertheless possible to obtain an expression in the form of an infinite series. In particular, defining $\hat{\xi} \triangleq \hat{h}^-/\hat{h}^+ = \tan^2\left(\hat{\delta}_{sy}/4\right)$ (for this case, $\hat{\xi} = \tan^2[\delta/4]$) and $\Lambda = U^+/U^-$, then after considerable effort and manipulation, the mean and variance of $\hat{R}$ can be evaluated in terms of the moments of Λ as

$$E\left\{\hat{R}\right\} = -1 + \left(1 - \hat{\xi}\right) \sum_{n=1}^{\infty} \hat{\xi}^{n-1} E\left\{\Lambda^n\right\}$$

$$\text{var}\left\{\hat{R}\right\} = \left(1 - \hat{\xi}\right)^2 \left[\sum_{n=2}^{\infty}(n-1)\hat{\xi}^{n-2} E\left\{\Lambda^n\right\} - \left(\sum_{n=1}^{\infty}\hat{\xi}^{n-1} E\left\{\Lambda^n\right\}\right)^2\right]$$

$$(6\text{-}27)$$

where

$$E\left\{\Lambda^n\right\} = \frac{\Gamma(N+n)\,\Gamma(N-n)}{\Gamma^2(N)}\,_1F_1\left(-n; N; -Nh^+R\right)\,_1F_1\left(n; N; -Nh^-R\right)$$

$$(6\text{-}28)$$

For small frequency error, i.e., $\hat{\xi}$ small, Eq. (6-27) can be simply approximated by

$$E\left\{\hat{R}\right\} = -1 + E\left\{\Lambda\right\} + \hat{\xi}\left[E\left\{\Lambda^2\right\} - E\left\{\Lambda\right\}\right]$$

$$\text{var}\left\{\hat{R}\right\} = \left(1 - 2\hat{\xi}\right) \times \text{var}\left\{\Lambda\right\} + 2\hat{\xi}\left[E\left\{\Lambda^3\right\} - E\left\{\Lambda\right\}E\left\{\Lambda^2\right\}\right]$$

$$(6\text{-}29)$$

Although not obvious from Eq. (6-27), it can be shown that the mean of the SNR estimator can be written in the form $E\{\hat{R}\} = R + O(1/N)$ and thus, for this case, the estimator is *asymptotically* (large N) unbiased.

•Case 2b: Frequency Uncertainty, Perfect Frequency Estimation, Half-Symbol Phase Compensation

$$\left(\omega \neq 0, \hat{\omega} = \omega, \omega_{sy} = \omega, \omega_s = 0 \Rightarrow \delta = \hat{\delta} \neq 0, \delta_{sy} = \hat{\delta}_{sy} = 0, \delta_s = \hat{\delta}_s = \delta\right)$$

Here we have $h^+ = \hat{h}^+ = W_{N_s}(\delta)$ for the sampled version or $h^+ = \hat{h}^+ = W(\delta)$ for the I&D version, $h^- = \hat{h}^- = 0$, and thus $\hat{R} = [(U^+ - U^-)/U^-]/\hat{h}^+$. Recognizing then that $\hat{h}^+\hat{R} + 1 = U^+/U^-$, the moments of $\hat{h}^+\hat{R}$ can be directly obtained from the moments of $\hat{R}$ of Case 0 by replacing R with h^+R. Thus,

$$E\left\{\hat{R}\right\} = \frac{1}{\hat{h}^+}\left[\frac{N}{N-1}h^+R + \frac{1}{N-1}\right]$$

$$(6\text{-}30)$$

$$\text{var}\left\{\hat{R}\right\} = \frac{1}{\left(\hat{h}^+\right)^2}\frac{1}{N-2}\left(\frac{N}{N-1}\right)^2\left[\left(1 + 2h^+R\right)\left(\frac{2N-1}{N}\right) + \left(h^+R\right)^2\right]$$

where for this case, as noted above, we can further set $h^+ = \hat{h}^+$. Once this is done in Eq. (6-30), then since $\hat{h}^+$ is known, we can once again completely remove the bias from the estimator by defining the bias-removed estimator $\hat{R}_0 = \left[(N-1)/N\right]R - 1/(N\hat{h}^+)$, whose mean is given by $E\{\hat{R}_0\} = R$ and whose variance is obtained from $\text{var}\{\hat{R}\}$ of Eq. (6-30) by multiplying it by $\left[(N-1)/N\right]^2$.

•Case 2c: Frequency Uncertainty, Perfect Frequency Estimation, Sample-by-Sample Phase Compensation

$$\left(\omega \neq 0, \hat{\omega} = \omega, \omega_{sy} = \omega_s = \omega \Rightarrow \delta = \hat{\delta} \neq 0, \delta_{sy} = \hat{\delta}_{sy} = \delta_s = \hat{\delta}_s = 0\right)$$

This case applies only to the sample-by-sample version of the SSME. In particular, we have $h^+ = \hat{h}^+ = 1, h^- = \hat{h}^- = 0$, and thus $\hat{R} = (U^+ - U^-)/U^-$, which is identical to the SSME of Case 0. Thus, the moments of $\hat{R}$ are given by Eq. (6-24).

●**Case 3a: Frequency Uncertainty, Imperfect Frequency Estimation, No Phase Compensation**

$$\left(\omega \neq 0, \hat{\omega} \neq \omega, \omega_{sy} = \omega_s = 0 \Rightarrow \delta, \hat{\delta} \neq 0, \delta_{sy} = \delta_s = \delta, \hat{\delta}_{sy} = \hat{\delta}_s = \hat{\delta}\right)$$

Here, $h^{\pm} = W_{N_s}(\delta)\left[1 \pm W_0(\delta)\right]/2, \hat{h}^{\pm} = W_{N_s}(\hat{\delta})\left[1 \pm W_0(\hat{\delta})\right]/2$ for the sampled version or $h^{\pm} = W(\delta)\left[1 \pm W_0(\delta)\right]/2, \hat{h}^{\pm} = W(\hat{\delta})\left[1 \pm W_0(\hat{\delta})\right]/2$ for the I&D version, and $\hat{R}$ is given by the generic form of Eq. (6-10). The method used to obtain the moments of the SNR estimator is analogous to that used for Case 2a. In particular, noting that for this case $\hat{\xi} = \tan^2\left(\hat{\delta}/4\right)$, the results are obtained from Eq. (6-27) by multiplying $E\{\hat{R}\}$ by $1/\hat{h}^+$ and $\text{var}\{\hat{R}\}$ by $\left(1/\hat{h}^+\right)^2$.

●**Case 3b: Frequency Uncertainty, Imperfect Frequency Estimation, Half-Symbol Phase Compensation**

$$\left(\omega \neq 0, \hat{\omega} \neq \omega, \omega_{sy} = \hat{\omega}, \omega_s = 0 \Rightarrow \delta, \hat{\delta} \neq 0, \delta_{sy} = \delta - \hat{\delta}, \hat{\delta}_{sy} = 0, \ \delta_s = \delta, \hat{\delta}_s = \hat{\delta}\right)$$

Here $h^{\pm} = W_{N_s}(\delta)\left[1 \pm W_0(\delta - \hat{\delta})\right]/2, \hat{h}^+ = W_{N_s}(\hat{\delta})$ for the sampled version or $h^{\pm} = W(\delta)\left[1 \pm W_0(\delta - \hat{\delta})\right]/2, \hat{h}^+ = W(\hat{\delta})$ for the I&D version, $\hat{h}^- = 0$, and once again $\hat{R} = \left[(U^+ - U^-)/U^-\right]/\hat{h}^+$. Hence, by analogy with Case 1, the mean and variance of the SNR estimator can be obtained from a scaled version of Eq. (6-26).

●**Case 3c: Frequency Uncertainty, Imperfect Frequency Estimation, Sample-by-Sample Phase Compensation**

$$\left(\omega \neq 0, \hat{\omega} \neq \omega, \omega_{sy} = \omega_s = \hat{\omega} \Rightarrow \delta, \hat{\delta} \neq 0, \delta_{sy} = \delta_s = \delta - \hat{\delta}, \hat{\delta}_{sy} = \hat{\delta}_s = 0\right)$$

This case applies only to the sample-by-sample version of the SSME. In particular, we have $h^{\pm} = W_{N_s}(\delta - \hat{\delta})\left[1 \pm W_0(\delta - \hat{\delta})\right]/2, \hat{h}^+ = 1, \hat{h}^- = 0$, and thus $\hat{R} = (U^+ - U^-)/U^-$, which is the form given in Eq. (6-12) and resembles Case 1. Thus, the moments of $\hat{R}$ are given by Eq. (6-26), using now the values of h^+ and h^- as are appropriate to this case.

6.4.2 Asymptotic Moment Evaluations

Despite having exact results, in many instances it is advantageous to have asymptotic results, particularly if their analytical form is less complex and as such lends insight into the their behavior in terms of the various system parameters. In this section, we provide approximate expressions for the mean and variance of the SSME by employing a Taylor series expansion of $g(U^+, U^-)$ in

Eq. (6-10), assuming that this function is smooth in the vicinity of the point $\left(E\{U^+\}, E\{U^-\}\right)$. With this in mind, the mean and variance of the estimate $\hat{R}$ are approximated by [10, p. 212]

$$E\{\hat{R}\} = g\left(E\left\{U^+\right\}, E\left\{U^-\right\}\right)$$

$$+ \frac{1}{2}\left(\text{var}\left\{U^+\right\}\frac{\partial^2 g}{\partial\left(U^+\right)^2} + \text{var}\left\{U^-\right\}\frac{\partial^2 g}{\partial\left(U^-\right)^2}\right) + O\left(\frac{1}{N^2}\right) \quad \text{(6-31)}$$

$$\text{var}\{\hat{R}\} = \left(\frac{\partial g}{\partial U^+}\right)^2 \text{var}\{U^+\} + \left(\frac{\partial g}{\partial U^-}\right)^2 \text{var}\{U^-\} + O\left(\frac{1}{N^2}\right)$$

In Eq. (6-31), all of the partial derivatives are evaluated at $\left(E\{U^+\}, E\{U^-\}\right)$. Ordinarily, there would be another term in these Taylor series expansions involving $\partial^2 g/\partial U^+\partial U^-$ and $\text{cov}\{U^+, U^-\}$. However, in our case, this term is absent in view of the independence of U^+ and U^-.

In Appendix 6-A, we derive explicit expressions for $E\{\hat{R}\}$ and $\text{var}\{\hat{R}\}$ based on the evaluations of the partial derivatives required in Eq. (6-31). The results of these evaluations are given below:

$$E\left\{\hat{R}\right\} = \frac{\left(h^+ - h^-\right)R}{\hat{h}^+ - \hat{h}^- + \left(\hat{h}^+ h^- - \hat{h}^- h^+\right)R}$$

$$+ \frac{1}{N}\frac{\left(\hat{h}^+ - \hat{h}^-\right)\left(\hat{h}^+ + \hat{h}^-\right)}{\left[\hat{h}^+ - \hat{h}^- + \left(\hat{h}^+ h^- - \hat{h}^- h^+\right)R\right]^3}$$

$$\times\left\{1 + \left(h^+ + h^- + \frac{\hat{h}^+ h^- + \hat{h}^- h^+}{\hat{h}^+ + \hat{h}^-}\right)R + 2h^+ h^- R^2\right\} + O\left(\frac{1}{N^2}\right)$$

$$\text{(6-32)}$$

and

$$\text{var}\left\{\hat{R}\right\} = \frac{1}{N} \frac{\left(\hat{h}^+ - \hat{h}^-\right)^2}{\left[\hat{h}^+ - \hat{h}^- + \left(\hat{h}^+ h^- - \hat{h}^- h^+\right) R\right]^4}$$

$$\times \left\{2 + 4\left(h^+ + h^-\right)R + \left[\left(h^+ + h^-\right)^2 + 6h^+ h^-\right]R^2 + 4h^+ h^-\left(h^+ + h^-\right)R^3\right\}$$

$$+ O\left(\frac{1}{N^2}\right) \tag{6-33}$$

It is now a simple matter to substitute in the various expressions for $h^\pm$ and $\hat{h}^\pm$ corresponding to the special cases treated in Section 6.1 to arrive at asymptotic closed-form expressions for the mean and variance of $\hat{R}$ for each of these cases. The results of these substitutions lead to the following simplifications:

•**Case 0: No Frequency Uncertainty**

$$E\{\hat{R}\} = R + \frac{1}{N}(1 + R) + O\left(\frac{1}{N^2}\right)$$

$$\tag{6-34}$$

$$\text{var}\left\{\hat{R}\right\} = \frac{1}{N}\left(2 + 4R + R^2\right) + O\left(\frac{1}{N^2}\right)$$

•**Case 1: Frequency Uncertainty, No Frequency Estimation (and thus No Phase Compensation)**

$$E\left\{\hat{R}\right\} = \frac{\left(h^+ - h^-\right)R}{1 + h^- R}$$

$$+ \frac{1}{N}\frac{1}{\left(1 + h^- R\right)^3}\left\{1 + \left(h^+ + 2h^-\right)R + 2h^+ h^- R^2\right\} + O\left(\frac{1}{N^2}\right)$$

$$\tag{6-35}$$

$$\text{var}\left\{\hat{R}\right\} = \frac{1}{N}\frac{1}{\left(1 + h^- R\right)^4}\left\{2 + 4\left(h^+ + h^-\right)R + \left[\left(h^+ + h^-\right)^2 + 6h^+ h^-\right]R^2\right.$$

$$\left. + 4h^+ h^-\left(h^+ + h^-\right)R^3\right\} + O\left(\frac{1}{N^2}\right)$$

where $h^{\pm} \; = \; W_{N_s}(\delta)\big[1 \pm W_0(\delta)\big]/2$ for the sampled version or $h^{\pm} \; = \; W(\delta)$ $\big[1 \pm W_0(\delta)\big]/2$ for the I&D version.

●**Case 2a: Frequency Uncertainty, Perfect Frequency Estimation, No Phase Compensation**

$$E\left\{\hat{R}\right\} =$$

$$R + \frac{1}{N} \frac{(h^+ + h^-)}{(h^+ - h^-)^2} \left\{ 1 + \left(h^+ + h^- + \frac{2h^+h^-}{h^+ + h^-} \right) R + 2h^+h^- R^2 \right\} + O\left(\frac{1}{N^2} \right)$$

$$(6\text{-}36)$$

$$\mathrm{var}\left\{\hat{R}\right\} = \frac{1}{N} \frac{1}{(h^+ - h^-)^2} \left\{ 2 + 4\left(h^+ + h^-\right) R + \left[\left(h^+ + h^-\right)^2 + 6h^+h^- \right] R^2 \right.$$

$$\left. + 4h^+h^- \left(h^+ + h^-\right) R^3 \right\} + O\left(\frac{1}{N^2} \right)$$

where $h^{\pm} \; = \; W_{N_s}(\delta)\big[1 \pm W_0(\delta)\big]/2$ for the sampled version or $h^{\pm} \; = \; W(\delta)$ $\big[1 \pm W_0(\delta)\big]/2$ for the I&D version.

●**Case 2b: Frequency Uncertainty, Perfect Frequency Estimation, Half-Symbol Phase Compensation**

$$E\left\{\hat{R}\right\} = R + \frac{1}{N} \frac{1}{h^+} \left(1 + h^+ R\right) + O\left(\frac{1}{N^2} \right)$$

$$(6\text{-}37)$$

$$\mathrm{var}\left\{\hat{R}\right\} = \frac{1}{N} \frac{1}{(h^+)^2} \left[2 + 4h^+ R + \left(h^+\right)^2 R^2 \right] + O\left(\frac{1}{N^2} \right)$$

where $h^+ = W_{N_s}(\delta)$ for the sampled version or $h^+ = W(\delta)$ for the I&D version.

•**Case 2c: Frequency Uncertainty, Perfect Frequency Estimation,
Sample-by-Sample Phase Compensation**

As was true for the exact results, the asymptotic mean and variance are again
the same as for Case 0.

•**Case 3a: Frequency Uncertainty, Imperfect Frequency Estimation,
No Phase Compensation**

No simplification of the results occurs here, and thus one merely applies
Eqs. (6-32) and (6-33), where $h^\pm = W_{N_s}(\delta)\left[1 \pm W_0(\delta)\right]/2, \hat{h}^\pm = W_{N_s}(\hat{\delta})$
$\left[1 \pm W_0(\hat{\delta})\right]/2$ for the sampled version or $h^\pm = W(\delta)\left[1 \pm W_0(\delta)\right]/2, \hat{h}^\pm =$
$W(\hat{\delta})\left[1 \pm W_0(\hat{\delta})\right]/2$ for the I&D version.

•**Case 3b: Frequency Uncertainty, Imperfect Frequency Estimation,
Half-Symbol Phase Compensation**

$$E\left\{\hat{R}\right\} = \frac{\left(h^+ - h^-\right)R}{\hat{h}^+ \left(1 + h^- R\right)} + \frac{1}{N}\frac{1}{\hat{h}^+}\frac{1}{\left(1 + h^- R\right)^3}$$

$$\times \left\{1 + \left(h^+ + 2h^-\right)R + 2h^+ h^- R^2\right\} + O\left(\frac{1}{N^2}\right)$$

$$(6\text{-}38)$$

$$\mathrm{var}\left\{\hat{R}\right\} = \frac{1}{N}\frac{1}{\left(\hat{h}^+\right)^2}\frac{1}{\left(1 + h^- R\right)^4}$$

$$\times \left\{2 + 4\left(h^+ + h^-\right)R + \left[\left(h^+ + h^-\right)^2 + 6h^+ h^-\right]R^2\right.$$

$$\left. + 4h^+ h^- \left(h^+ + h^-\right)R^3\right\} + O\left(\frac{1}{N^2}\right)$$

where $h^\pm = W_{N_s}(\delta)\left[1 \pm W_0\left(\delta - \hat{\delta}\right)\right]/2, \hat{h}^+ = W_{N_s}(\hat{\delta})$ for the sampled version or
$h^\pm = W(\delta)\left[1 \pm W_0\left(\delta - \hat{\delta}\right)\right]/2, \hat{h}^+ = W(\hat{\delta})$ for the I&D version.

●**Case 3c: Frequency Uncertainty, Imperfect Frequency Estimation, Sample-by-Sample Phase Compensation**

$$E\{\hat{R}\} = \frac{(h^+ - h^-)R}{1 + h^- R} + \frac{1}{N} \frac{1}{(1 + h^- R)^3}$$

$$\times \{1 + (h^+ + 2h^-)R + 2h^+ h^- R^2\} + O(\frac{1}{N^2})$$

(6-39)

$$\text{var}\{\hat{R}\} = \frac{1}{N} \frac{1}{(1 + h^- R)^4} \{2 + 4(h^+ + h^-)R + \left[(h^+ + h^-)^2 + 6h^+ h^-\right] R^2$$

$$+ 4h^+ h^- (h^+ + h^-)R^3\} + O\left(\frac{1}{N^2}\right)$$

where $h^{\pm} = W_{N_s}(\delta - \hat{\delta}) \left[1 \pm W_0(\delta - \hat{\delta})\right]$.

6.4.2.1. Numerical Results and Comparisons. To compare the performances of the estimator corresponding to the various cases just discussed, we first define a parameter $\hat{N} = N\text{var}\{\hat{R}\}/R^2$ (or in the cases where a bias-removed estimator is possible, $\hat{N}_0 = N\text{var}\{\hat{R}_0\}/R^2$), which measures the number of symbols that are needed to achieve a fractional mean-squared estimation error of 100 percent using that estimator. Then, if one wishes to achieve a smaller fractional mean-squared estimation error, say $\text{var}\{\hat{R}\}/R^2 = \varepsilon^2$ (or $\text{var}\{\hat{R}_0\}/R^2 = \varepsilon^2$), then the required number of symbols to achieve this level of performance would simply be $N_{req}(\varepsilon^2) = \hat{N}/\varepsilon^2$ (or $N_{req}(\varepsilon^2) = \hat{N}_0/\varepsilon^2$). As an example, consider the bias-removed SNR estimator for Case 2b for which $\hat{N}_0$ can be determined from Eq. (6-30) as

$$\hat{N}_0 = \frac{\left(1 - \frac{1}{2N}\right)\left(\frac{2}{(h^+ R)^2} + \frac{4}{h^+ R}\right) + 1}{1 - \frac{2}{N}}$$

(6-40)

Clearly, the above interpretation of the meaning of $\hat{N}_0$ is a bit circular in that $\hat{N}_0$ of Eq. (6-40) depends on N. However, this dependence is mild for reasonable values of N. Thus, to a good approximation one can replace $\hat{N}_0$ by its limiting value $\hat{N}_0^*$ corresponding to $N = \infty$, in which case the required number of symbols

to achieve a fractional mean-squared estimation of ε^2 would approximately be given by

$$N_{req}\left(\varepsilon^2\right) \cong \frac{\hat{N}_0^*}{\varepsilon^2}$$

$$\hat{N}_0^* = \frac{2}{(h^+R)^2} + \frac{4}{h^+R} + 1$$

(6-41)

Alternatively, for this case one uses the exact expression for the fractional mean-squared estimation error to solve directly for $N_{req}\left(\varepsilon^2\right)$. In particular, dividing Eq. (6-30) (multiplied by $\left[(N-1)/N\right]^2$) by R^2 and equating the result to ε^2 results in a quadratic equation in N whose solution can be exactly expressed as

$$N_{req}\left(\varepsilon^2\right) = \left(1 + \frac{\hat{N}_0^*}{2\varepsilon^2}\right)\left[1 + \sqrt{1 - \frac{\left(\hat{N}_0^* - 1\right)2\varepsilon^2}{\left(\hat{N}_0^* + 2\varepsilon^2\right)^2}}\right]$$

(6-42)

Since the value of the negative term in the square root is less than $2\varepsilon^2/\hat{N}_0^*$, an approximate (for small ε^2) upper bound on Eq, (6-42) is given by

$$N_{req}\left(\varepsilon^2\right) < \left(1 + \frac{\hat{N}_0^*}{2\varepsilon^2}\right)\left[1 + \sqrt{1 - \frac{2\varepsilon^2}{\hat{N}_0^*}}\right] \cong \left(1 + \frac{\hat{N}_0^*}{2\varepsilon^2}\right)\left(2 - \frac{\varepsilon^2}{\hat{N}_0^*}\right) \cong \frac{\hat{N}_0^*}{\varepsilon^2} + \frac{3}{2}$$

(6-43)

Thus, we see that the exact number of requisite symbols is not more than two extra symbols beyond the number that would be obtained from the approximate number in Eq. (6-41).

Figure 6-4 is a plot of $\hat{N}_0$ versus R in decibels with N as a parameter for the biased-removed estimator of Case 0, where the results are determined from Eq. (6-25). We observe that a value of $N = 50$ is virtually sufficient to approach the asymptotic value $\hat{N}_0^* = 1 + 2(1 + 2R)/R^2$. For the biased-removed estimator of Case 2b, a plot of $\hat{N}_0$ versus h^+R in decibels would be identical to Fig. 6-4, in accordance with Eq. (6-30) and the comments below this equation. Thus, the degradation in performance when frequency uncertainty is present but is perfectly estimated and fully compensated for is reflected in a horizontal shift of the curves in Fig. 6-4 to the right by an amount equal to h^+. Equivalently, a
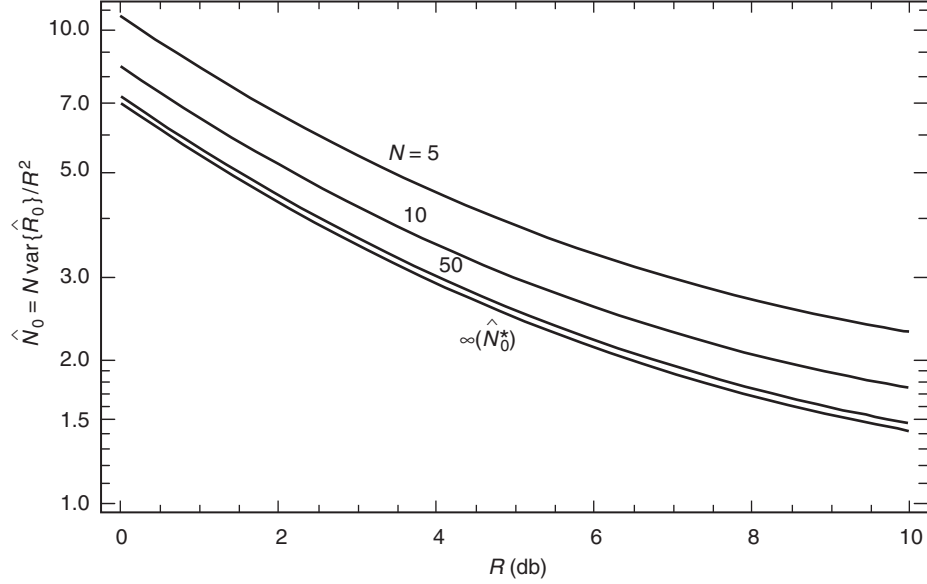
Fig. 6-4. Case 0: No frequency offset, perfect frequency estimate, no phase compensation.

larger number of symbols is now required to achieve the same SNR estimation accuracy as for the case of no frequency uncertainty.

For Case 3b where the frequency uncertainty estimate is imperfect but is still used for compensation, the asymptotic (N large) behavior is obtained from Eq. (6-33). In particular, for $N \rightarrow \infty$,

$$E\{\hat{R}\} = \frac{(h^+ - h^-)R}{\hat{h}^+(1 + h^- R)}$$

$$\hat{N}^* = \lim_{N \rightarrow \infty} \frac{N\mathrm{var}(\hat{R})}{R^2} = \frac{1}{\left(\hat{h}^+\right)^2 (1 + h^- R)^4} \left\{ \frac{2}{R^2} + \frac{4(h^+ + h^-)}{R} \right. \quad (6\text{-}44)$$

$$\left. + (h^+ + h^-)^2 + 6h^+ h^- + 4h^+ h^- (h^+ + h^-)R \right\}$$

Figures 6-5 and 6-6 are plots of $E\{\hat{R}\}$ versus R in decibels for fixed $\delta/(2\pi) = fT$ and fractional frequency estimation error $(\delta - \hat{\delta})/\delta$ as a parameter varying between -10 percent and 10 percent. We observe that for a relative frequency
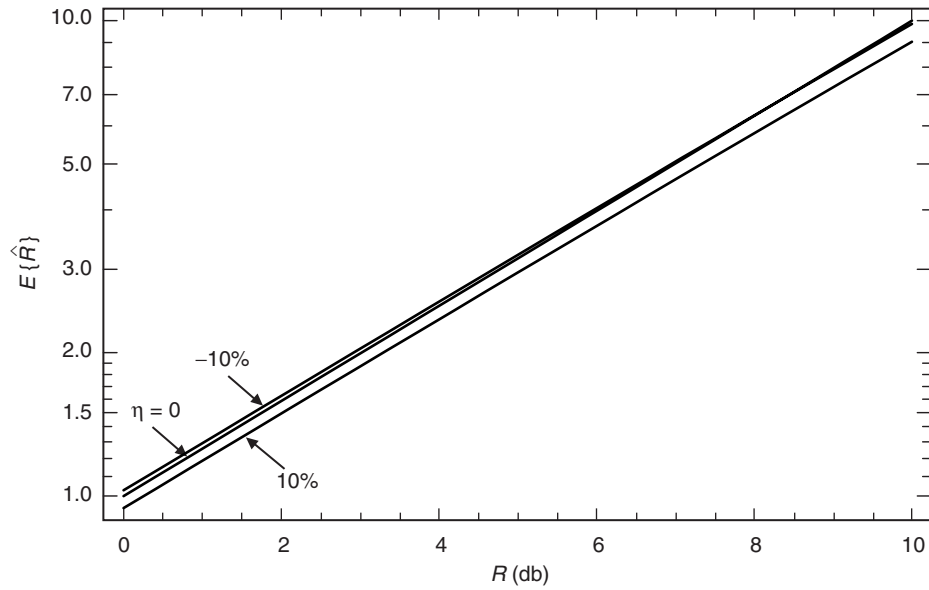
Fig. 6-5. Mean of estimator versus SNR in decibels; Case 3b; frequency offset, imperfect frequency estimate, half-symbol phase compensation; relative frequency uncertainty $\delta/(2\pi) = fT = 0.5$**, fractional frequency error** $\eta = 0, -10\%, 10\%$**.**
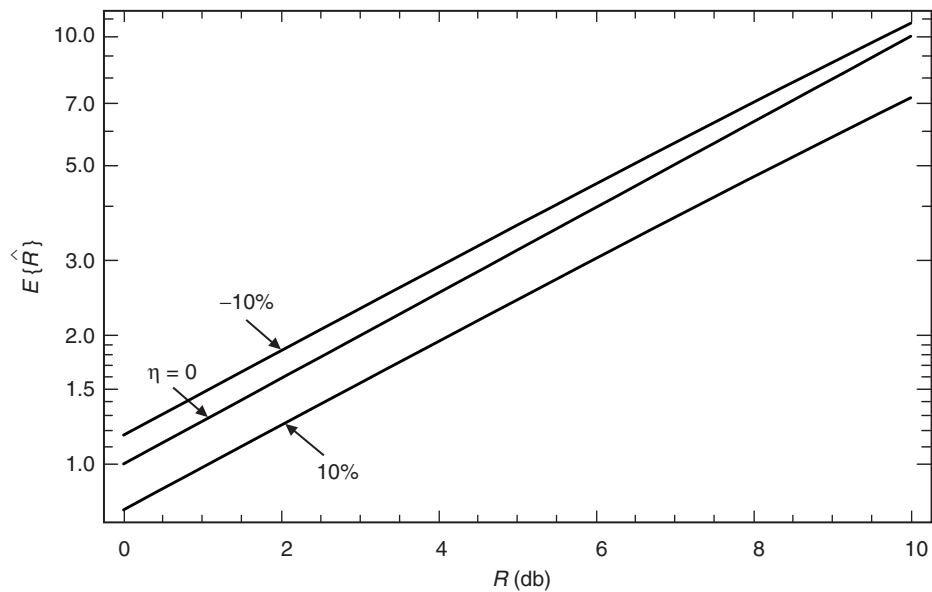

Fig. 6-6. Mean of estimator versus SNR in decibels; Case 3b; frequency offset, imperfect frequency estimate, half-symbol phase compensation; relative frequency uncertainty $\delta/(2\pi) = fT = 1.0$**, fractional frequency error** $\eta = 0, -10\%, 10\%$**.**

uncertainty of half a cycle ($\delta/(2\pi) = 0.5$), the amount of bias is quite small over the range of frequency estimation errors considered. When the relative frequency error increases to a full cycle ($\delta/(2\pi) = 1.0$), then the sensitivity of the bias to frequency estimation error becomes more pronounced. Also, it can be observed that, for a fixed frequency offset, the bias is not a symmetric function of the frequency estimation error. Figure 6-7 is a plot of $\hat{N}^*$ versus R in decibels for a fixed fractional estimation error $\eta = 5$ percent and $\delta/(2\pi) = fT$ as a parameter varying between 0.5 and 0.9. These curves are analogous to the ones in Fig. 6-4 with the purpose of demonstrating the sensitivity of the number of symbols required for a given level of mean-squared error performance to frequency uncertainty and estimation error.

6.5 SNR Estimation in the Presence of Symbol Timing Error

Until now we have considered the performance of the SSME estimator assuming that the symbol timing was either known or could be perfectly estimated. In this section, we extend the previous results corresponding to the I&D version[3]
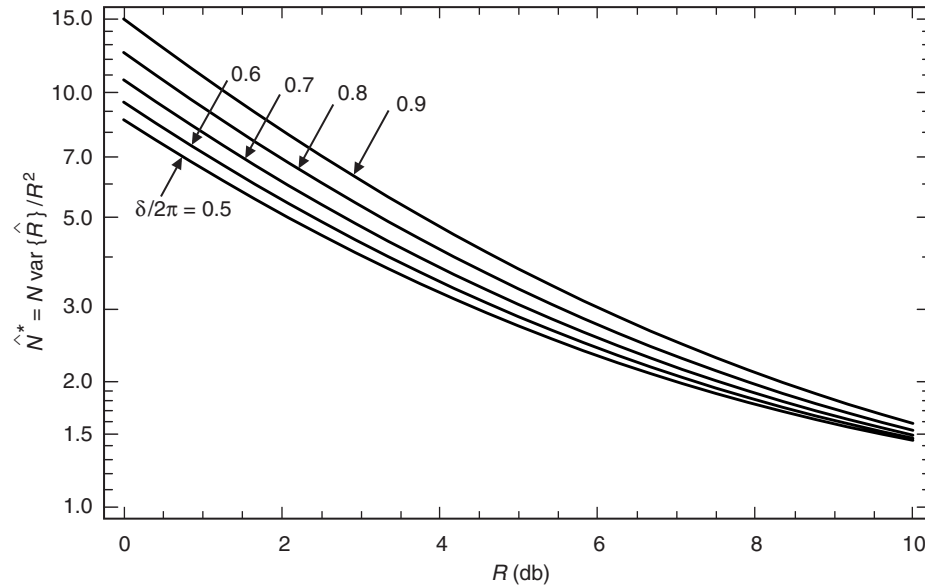

Fig. 6-7. Case 3b: frequency offset, imperfect frequency estimate, half-symbol phase compensation; fractional frequency uncertainty error η = 5%.

---

[3] Extension of the results to the sampled version is straightforward and is omitted for the sake of brevity.

of the SSME to the case where symbol timing is imperfect but the carrier frequency is known[4]—carrier phase is still assumed unknown. Clearly, although in any realistic system implementation both frequency uncertainty and symbol timing error will exist simultaneously, treating them as separate entities gives us a means of obtaining analytical results for their individual behavior and the sensitivity of system performance to each. The true degradation in the performance of the SNR estimator in their joint presence must be determined from simulation results.

6.5.1 Signal Model and Formation of the Estimator

Corresponding to the complex baseband received signal in the kth interval $(k-1)T \leq t < kT$, as described by Eq. (6-13), in the presence of a symbol timing error εT (for the moment we assume $0 \leq \varepsilon \leq 1/2$), the outputs of the first and second half-symbol I&Ds are given by

$$Y_{\alpha k} = m d_k \frac{1}{T} \int_{(k-1+\varepsilon)T}^{(k-1/2+\varepsilon)T} e^{j\phi} dt + \frac{1}{T} \int_{(k-1+\varepsilon)T}^{(k-1/2+\varepsilon)T} n(t)\, dt = \frac{m d_k}{2} e^{j\phi} + n_{\alpha k}$$

$$Y_{\beta k} = m d_k \frac{1}{T} \int_{(k-1/2+\varepsilon)T}^{kT} e^{j\phi} dt + m d_{k+1} \frac{1}{T} \int_{kT}^{(k+\varepsilon)T} e^{j(\omega t + \phi)} dt$$

$$(6\text{-}45)$$

$$+ \frac{1}{T} \int_{(k-1/2+\varepsilon)T}^{(k+\varepsilon)T} n(t)\, dt$$

$$= m e^{j\phi} \left[d_k \left(\frac{1}{2} - \varepsilon \right) + d_{k+1} \varepsilon \right] + n_{\beta k}$$

Independent of the symbol timing offset εT, the complex noise variables $n_{\alpha k}$ and $n_{\beta k}$ are still zero-mean Gaussian with variance $\sigma^2/2$ for each real and imaginary component. From the observables in Eq. (6-45), we again form the sum and difference variables

$$u_k^{\pm} = Y_{\alpha k} \pm Y_{\beta k} = m e^{j\phi} \left[d_k \left(\frac{1}{2} \pm \left(\frac{1}{2} - \varepsilon \right) \right) \pm d_{k+1} \varepsilon \right] + n_{\alpha k} \pm n_{\beta k} \triangleq s_k^{\pm} + n_k^{\pm}$$

$$(6\text{-}46)$$

---

[4] Later on, we shall consider one particular system model that allows for frequency uncertainty with perfect compensation and that falls in the same mathematical framework.

It is straightforward to show that the normalized squared norm of the signal components can be evaluated as

$$h_k^+ \triangleq \frac{\left|s_k^+\right|^2}{m^2} = 1 - 4\varepsilon\left(1 - \varepsilon\right)\sin^2\left(\frac{\Delta\phi_{k+1}}{2}\right)$$

$$(6\text{-}47)$$

$$h_k^- \triangleq \frac{\left|s_k^-\right|^2}{m^2} = 4\varepsilon^2\sin^2\left(\frac{\Delta\phi_{k+1}}{2}\right)$$

where $\Delta\phi_{k+1} = \phi_{k+1} - \phi_k$ denotes the transition in the data symbol phase in going from the kth symbol interval to the k+1st. Note that, as in the previous publication on the subject [6], the parameters $h_k^{\pm}$ do not depend on the random carrier phase ϕ; however, unlike these previous investigations, they do now depend on the data via the transitions in the symbol phase sequence. Furthermore, it is not obvious at this point (this will become clear shortly) to what extent $h_k^{\pm}$ is independent of the order M of the M-PSK modulation. For $-1/2 \leq \varepsilon \leq 0$, the analogous relations to Eq. (6-47) are

$$h_k^+ = 1 + 4\varepsilon\left(1 + \varepsilon\right)\sin^2\left(\frac{\Delta\phi_k}{2}\right)$$

$$(6\text{-}48)$$

$$h_k^- = 4\varepsilon^2\sin^2\left(\frac{\Delta\phi_k}{2}\right)$$

Next, we calculate N-symbol averages of the squared norms of the half-symbol sums to produce $U^{\pm}$ as in Eq. (6-6). Once again we make the key observation (as previously proved) that, now conditioned on the data symbol transition sequence, the observables U^+ and U^- are independent RVs. Defining, as before, the true SNR by $R = m^2/2\sigma^2$, then after averaging over the uniform distribution of the data symbol transitions around the circle defining the M-PSK constellation, it is straightforward (although a bit laborious) to show that their means and variances are, analogous to Eq. (6-8), given by

$$E\left\{U^{\pm}\right\} = 2\sigma^2\left(1 + \bar{h}^{\pm}R\right)$$

$$(6\text{-}49)$$

$$\mathrm{var}\left\{U^{\pm}\right\} = \frac{4}{N}\sigma^4\left(1 + 2\bar{h}^{\pm}R + \mathrm{var}\left\{h^{\pm}\right\}R^2\right)$$

where the overbar on $h^{\pm}$ denotes the above-mentioned statistical averaging over the data symbol transition sequence and the subscript k has been dropped since the statistical averages do not depend on k. Making use of the relations

$$\overline{\sin^2\left(\frac{\Delta\phi_k}{2}\right)} = \frac{1}{M}\sum_{k=0}^{M-1}\sin^2\frac{k\pi}{M} = \frac{1}{2}$$

$$\overline{\sin^4\left(\frac{\Delta\phi_k}{2}\right)} = \frac{1}{M}\sum_{k=0}^{M-1}\sin^4\frac{k\pi}{M} = \begin{cases} \dfrac{1}{2}, & M = 2 \\[2mm] \dfrac{3}{8}, & M > 2 \end{cases}$$

$$(6\text{-}50)$$

we have from Eqs. (6-47) and (6-48) that

$$\bar{h}^+ = 1 - 2\left|\varepsilon\right|\left(1 - \left|\varepsilon\right|\right)$$

$$\bar{h}^- = 2\left|\varepsilon\right|^2$$

$$(6\text{-}51)$$

and

$$\operatorname{var}\left\{h^+\right\} = \begin{cases} 4\left|\varepsilon\right|^2\left(1 - \left|\varepsilon\right|\right)^2, & M = 2 \\[2mm] 2\left|\varepsilon\right|^2\left(1 - \left|\varepsilon\right|\right)^2, & M > 2 \end{cases}$$

$$\operatorname{var}\left\{h^-\right\} = \begin{cases} 4\left|\varepsilon\right|^4, & M = 2 \\[2mm] 2\left|\varepsilon\right|^4, & M > 2 \end{cases}$$

$$(6\text{-}52)$$

Finally, since from the first relation in Eq. (6-49) R is expressible as

$$R = \frac{E\left\{U^+\right\} - E\left\{U^-\right\}}{\bar{h}^+ E\left\{U^-\right\} - \bar{h}^- E\left\{U^+\right\}}$$

$$(6\text{-}53)$$

then, as in the perfect symbol timing case, the general form of the ad hoc SSME $\hat{R}$ is obtained by substituting the sample values $U^{\pm}$ for their expected values and the estimates $\hat{\bar{h}}^{\pm}$ for their true values, namely,

$$\hat{R} = \frac{U^+ - U^-}{\hat{\bar{h}}^+ U^- - \hat{\bar{h}}^- U^+}$$

$$(6\text{-}54)$$

where $\hat{\bar{h}}^{\pm}$ are obtained from $\bar{h}^{\pm}$, defined in Eq. (6-51) by substituting the symbol timing estimate $\hat{\varepsilon}$ for ε. Actually, in view of Eq. (6-51), it is necessary to have only an estimate of the magnitude of ε. A method for obtaining such an estimate based on the same statistics used to form the SNR estimator will be discussed elsewhere in the text.

6.5.2 Mean and Variance of the SNR Estimator

In this section, we evaluate the mean and variance of $\hat{R}$ using the same techniques as in previous sections of the chapter. Since, for $|\hat{\varepsilon}| > 0$, $\hat{\bar{h}}^{\pm}$ are both non-zero, obtaining an exact compact closed-form expression is difficult. Nevertheless, it is possible to obtain a closed-form expression in the form of an infinite series. In particular, defining $\hat{\xi} \triangleq \hat{\bar{h}}^{-}/\hat{\bar{h}}^{+}$ and $\Lambda \triangleq U^{+}/U^{-}$, we can express $\hat{R}$ of Eq. (6-54) in the form

$$\hat{R} = \frac{1}{\hat{\bar{h}}^{+}} \frac{\Lambda - 1}{1 - \hat{\xi}\Lambda} = \frac{1}{\hat{\bar{h}}^{+}} (\Lambda - 1) \sum_{n=0}^{\infty} \left(\hat{\xi}\Lambda\right)^{n} = \frac{1}{\hat{\bar{h}}^{+}} \left[-1 + \left(1 - \hat{\xi}\right) \sum_{n=1}^{\infty} \hat{\xi}^{n-1}\Lambda^{n}\right]$$

(6-55)

Thus, the mean of $\hat{R}$ is expressed in terms of the moments of Λ by

$$E\left\{\hat{R}\right\} = \frac{1}{\hat{\bar{h}}^{+}} \left[-1 + \left(1 - \hat{\xi}\right) \sum_{n=1}^{\infty} \hat{\xi}^{n-1} E\left\{\Lambda^{n}\right\}\right]$$

(6-56)

Similarly, the variance of $\hat{R}$ can be evaluated in terms of the moments of Λ as

$$\text{var}\left\{\hat{R}\right\} = \frac{\left(1 - \hat{\xi}\right)^{2}}{\left(\hat{\bar{h}}^{+}\right)^{2}} \left[\sum_{n=2}^{\infty} (n - 1)\,\hat{\xi}^{n-2} E\left\{\Lambda^{n}\right\} - \left(\sum_{n=1}^{\infty} \hat{\xi}^{n-1} E\left\{\Lambda^{n}\right\}\right)^{2}\right]$$ (6-57)

An expression for the moments of Λ in terms of $h^{\pm}$ can be obtained from Eq. (6-23) and [8, Eq. (2.47)] as

$$E\left\{\Lambda^{n}\right\} = \frac{\Gamma\left(N + n\right)\Gamma\left(N - n\right)}{\Gamma^{2}\left(N\right)} {}_{1}F_{1}\left(-n; N; -Nh^{+}R\right) {}_{1}F_{1}\left(n; N; -Nh^{-}R\right)$$

(6-58)

Since, in accordance with Eqs. (6-47) and (6-48), $h^{\pm}$ are now functions of the data phase symbol transitions $\Delta\phi_{k+1}$, we must further average Eq. (6-58) over the uniformly distributed statistics of this RV in the same manner as we did previously in arriving at $\bar{h}^{\pm}$. The difference here is that $h^{\pm}$ are embedded as arguments of the hypergeometric function, and thus the average cannot be obtained in closed form. Nevertheless, the appropriate modification of Eq. (6-58) now becomes

$$E\left\{\Lambda^n\right\} = \frac{\Gamma\left(N+n\right)\Gamma\left(N-n\right)}{\Gamma^2\left(N\right)}\overline{{}_1F_1\left(-n;N;-Nh^+R\right){}_1F_1\left(n;N;-Nh^-R\right)}^{\Delta\phi}$$

$$(6\text{-}59)$$

where, for M-PSK, $\Delta\phi$ takes on values $2k\pi/M, k = 0, 1, 2, \cdots, M-1$, each with probability $1/M$.

For small symbol timing offset, i.e., $\hat{\xi}$ small, Eqs. (6-56) and (6-57) can be simply approximated by

$$E\left\{\hat{R}\right\} = \left(\frac{1}{\hat{\bar{h}}^+}\right)\left[-1 + E\left\{\Lambda\right\} + \hat{\xi}\left(E\left\{\Lambda^2\right\} - E\left\{\Lambda\right\}\right)\right]$$

$$(6\text{-}60)$$

$$\mathrm{var}\left\{\hat{R}\right\} = \left(\frac{1}{\hat{\bar{h}}^+}\right)^2\left[\left(1 - 2\hat{\xi}\right)\times\mathrm{var}\left\{\Lambda\right\} + 2\hat{\xi}\left(E\left\{\Lambda^3\right\} - E\left\{\Lambda\right\}E\left\{\Lambda^2\right\}\right)\right]$$

and thus only the first few moments of Λ need be evaluated.

6.6 A Generalization of the SSME Offering Improved Performance

In this section, we consider a modification of the SSME structure that provides improved performance in the sense of lowering the variance of the SNR estimator. To simplify matters, we begin the discussion by considering the ideal case of no frequency uncertainty. Also, for the sake of brevity, we investigate only the I&D version. Suffice it to say that the generalization is readily applied to the sampled version in an obvious manner.

To motivate the search for an SSME structure with improved performance, we define a measure of "quality" of the SNR estimator by its own SNR, namely, $Q = \left(E\{\hat{R}\}\right)^2/\mathrm{var}\{\hat{R}\}$. For large N and large R, we have from Eq. (6-24) that $E\{\hat{R}\} = R, \mathrm{var}\{\hat{R}\} = R^2/N$, and thus $Q = N$. Thus, we observe that for fixed

observation time, the quality of the conventional SSME does not continue to improve as the true SNR, R, increases, but instead saturates to a fixed value. With this in mind, we seek to modify the SSME such that for a fixed observation time the quality of the estimator continues to improve with increasing SNR.

Suppose now that instead of subdividing each data symbol interval T into two halves, we subdivide it into $2L$ subintervals of equal length $T/(2L)$ and use the integrations of the complex-valued received signal plus noise in successive pairs of these intervals to form the SNR estimator. In effect, we are estimating the symbol SNR of a data sequence at L times the actual data rate. This data sequence is obtained by repeating each original data symbol L times to form L consecutive shorter symbols, and thus it is reasonable to refer to L as an *over-sampling factor*. For a given total observation time (equivalently, a given total number of original symbols N), there are LN short symbols corresponding to the higher data rate, and their symbol SNR is $r = R/L$. Since the SSME is completely independent of the data sequence, the new estimator, denoted by $\hat{r}_L$, is just an SSME of the SNR $r = R/L$ of the short symbols, based on observing LN short symbols, each split into half. Thus, the mean and variance of $\hat{r}_L$ are computed by simply replacing N by LN and R by R/L in Eq. (6-24), which is rewritten here for convenience as

$$E\left\{\hat{R}\right\} = R + \frac{R+1}{N-1}$$

(6-61)

$$\mathrm{var}\left\{\hat{R}\right\} = \frac{1}{N-2}\left(\frac{N}{N-1}\right)^2\left[(2+4R)\left(\frac{N-1/2}{N}\right) + R^2\right]$$

Since, however, we desire an estimate of R, not $r = R/L$, we define $\hat{R}_L = L\hat{r}_L$ and write the corresponding expressions for the mean and variance of $\hat{R}_L$:

$$E\left\{\hat{R}_L\right\} = L\left[\frac{R}{L} + \frac{R/L+1}{LN-1}\right] = R + \frac{R+L}{LN-1}$$

(6-62)

$$\mathrm{var}\left\{\hat{R}_L\right\} = \frac{L^2}{LN-2}\left(\frac{LN}{LN-1}\right)^2\left[\left(2+\frac{4R}{L}\right)\left(\frac{LN-1/2}{LN}\right) + \left(\frac{R}{L}\right)^2\right]$$

With this notation, the original SSME is simply $\hat{R} = \hat{R}_1$, and the performance expressions in Eq. (6-62) are valid for any positive integer $L \in \{1, 2, 3, \cdots\}$. For large N, i.e., $N \gg 1$, the mean and variance in Eq. (6-62) simplify within $O(1/N^2)$ to

$$E\left\{\hat{R}_L\right\} = R + \frac{R+L}{LN}$$

$$\text{var}\left\{\hat{R}_L\right\} = \frac{L}{N}\left(2 + \frac{4R}{L} + \frac{R^2}{L^2}\right)$$

(6-63)

For the remainder of this section, we base our analytic derivations on the asymptotic expressions in Eq. (6-63).

For small enough R, we can ignore the R and R^2 terms in the variance expression, and the smallest estimator variance is achieved for $L = 1$. In this case, $\hat{R} = \hat{R}_1$ outperforms (has smaller variance than) $\hat{R}_L$ for $L > 1$, approaching a $10\log_{10} L$ dB advantage as $R \to 0$. However, at large enough R for any fixed L, the reverse situation takes place. In particular, retaining only the R^2 term in Eq. (6-63) for sufficiently large R/L, we see that $\hat{R}_L$ offers a $10\log_{10} L$ dB advantage over $\hat{R}$ in this limit. This implies that for small values of R, a half-symbol SSME (i.e., $L = 1$) is the preferred implementation, whereas beyond a certain critical value of R (to be determined shortly) there is an advantage to using values of $L > 1$. In general, for any given R, there is an optimum integer $L = L_*(R)$ that minimizes the variance in Eq. (6-63). We denote the corresponding optimum estimator by $\hat{R}_*$. We show below that, unlike the case of the estimator $\hat{R}_L$ defined for a fixed L, the optimized estimator $\hat{R}_*$ requires proportionally more subdivisions of the true symbol interval as R gets large. As a result, the R^2/L^2 term in Eq. (6-63) does not totally dominate the variance for $R \gg L$, and the amount of improvement at high SNR differs from the $10\log_{10} L$ dB improvement calculated for an arbitrary fixed choice of L and $R \gg L$.

For the moment we ignore the fact that L must be an integer, and minimize the variance expression in Eq. (6-63) over continuously varying *real-valued* L. We define an optimum real-valued $L = L_\bullet(R)$, obtained by differentiating the variance expression of Eq. (6-63) with respect to L and equating the result to zero, as

$$L_\bullet(R) = \frac{R}{\sqrt{2}}$$

(6-64)

and a corresponding *fictitious* SNR estimator $\hat{R}_\bullet$ that "achieves" the minimum variance calculated by substituting Eq. (6-64) into the asymptotic variance expression of Eq. (6-63),

$$\text{var}\left\{\hat{R}_\bullet\right\} = \frac{R}{N}\left(4 + 2\sqrt{2}\right)$$

(6-65)

The minimum variance shown in Eq. (6-65) can be achieved only by a realizable estimator for values of R that yield an integer $L_\bullet(R)$ as defined by Eq. (6-64). Nevertheless, it serves as a convenient benchmark for comparisons with results corresponding to the optimized realistic implementation $\hat{R}_*$. For example, from Eqs. (6-63) and (6-65) we see that the ratio of the asymptotic variance achieved by any given realizable estimator $\hat{R}_L$ to that achieved by the fictitious estimator $\hat{R}_\bullet$ is a simple function of the short symbol SNR r, not of R and L separately. In particular,

$$\frac{\text{var}\left\{\hat{R}_L\right\}}{\text{var}\left\{\hat{R}_\bullet\right\}} = \frac{2/r + 4 + r}{4 + 2\sqrt{2}} \tag{6-66}$$

The numerator of Eq. (6-66) is a convex $\cup$ function of r, possessing a unique minimum at $r = \sqrt{2}$, at which point the ratio in Eq. (6-66) evaluates to unity. This result is not surprising since, from Eq. (6-64), $r = \sqrt{2}$ is the optimality condition defining the fictitious estimator $\hat{R}_\bullet$. For $r > \sqrt{2}$ or $r < \sqrt{2}$, the ratio in Eq. (6-66) for any fixed value of L grows without bound.

Before going on, let us examine how allowing L to vary with R in an optimum fashion in accordance with Eq. (6-64) has achieved the improvement in "quality" we previously set out to obtain. In particular, since for large N and large R we have $E\{R_\bullet\} = R$ and from Eq. (6-65) $\text{var}\{\hat{R}_\bullet\} = (R/N)\left(4 + 2\sqrt{2}\right)$, then it immediately follows that $Q = \left(E\{\hat{R}\}\right)^2/\text{var}\{\hat{R}\} = NR/(4 + 2\sqrt{2})$, which demonstrates that, for a fixed observation time, the quality of the estimator now increases linearly with true SNR.

We return now to the realistic situation where L must be an integer, but can vary with R or r. Since the variance expression in Eq. (6-63) is convex $\cup$ in L, we can determine whether $\hat{R}_L$ is optimum for a given R by simply comparing its performance to that of its nearest neighbors, $\hat{R}_{L-1}$ and $\hat{R}_{L+1}$. We find that $\hat{R}_L$ is optimum over a continuous range $R \in \left[R_L^-, R_L^+\right]$, where $R_1^- = 0$, $R_{L+1}^- = R_L^+$, and the upper boundary point is determined by equating the variance expressions in Eq. (6-63) for $\hat{R}_L$ and $\hat{R}_{L+1}$:

$$R_L^+ = \sqrt{2L\left(L + 1\right)} \tag{6-67}$$

Thus, the optimum integer $L_*(R)$ is evaluated as

$$L_*(R) = L, \quad \text{if} \quad \sqrt{2L\left(L - 1\right)} \le R \le \sqrt{2L\left(L + 1\right)} \tag{6-68}$$

In particular, we see that $\hat{R}_1$ is optimum in the region $0 \leq R \leq 2$, implying no improvement over the original SSME for these values of R. For values of R in the region $2 \leq R < 2\sqrt{3}$, one should use $\hat{R}_2$ (i.e., an estimator based on pairs of quarter-symbol integrations), and in general one should use $\hat{R}_L$ when $\sqrt{2L(L-1)} \leq R \leq \sqrt{2L(L+1)}$. For R in this interval, the improvement factor $I(R)$ (reduction in variance) achieved by the new optimized estimator relative to the conventional half-symbol SSME $\hat{R} = \hat{R}_1$ is calculated as

$$I(R) = \frac{\text{var}\left\{\hat{R}\right\}}{\text{var}\left\{\hat{R}_*\right\}} = \frac{2 + 4R + R^2}{L\left(2 + \dfrac{4R}{L} + \dfrac{R^2}{L^2}\right)}, \quad \sqrt{2L(L-1)} \leq R \leq \sqrt{2L(L+1)}$$

(6-69)

We have already seen that $I(R) = 1$ for R ranging from 0 to 2, whereupon it becomes better to use $\hat{R}_2$, allowing $I(R)$ to increase monotonically to a value of $\left(7 + 4\sqrt{3}\right)/\left(5 + 4\sqrt{3}\right) = 1.168$ (equivalent to 0.674 dB) at $R = 2\sqrt{3}$. Continuing on, in the region $2\sqrt{3} \leq R < 2\sqrt{6}$, one should use $\hat{R}_3$, whereupon $I(R)$ continues to increase monotonically to a value of $\left(13 + 4\sqrt{6}\right)/\left(7 + 4\sqrt{6}\right) = 1.357$ (equivalent to 1.326 dB) at $R = 2\sqrt{6}$. Figure 6-8 is a plot of $I(R)$ versus R, as determined from Eq. (6-69). Note that while $I(R)$ is a continuous function
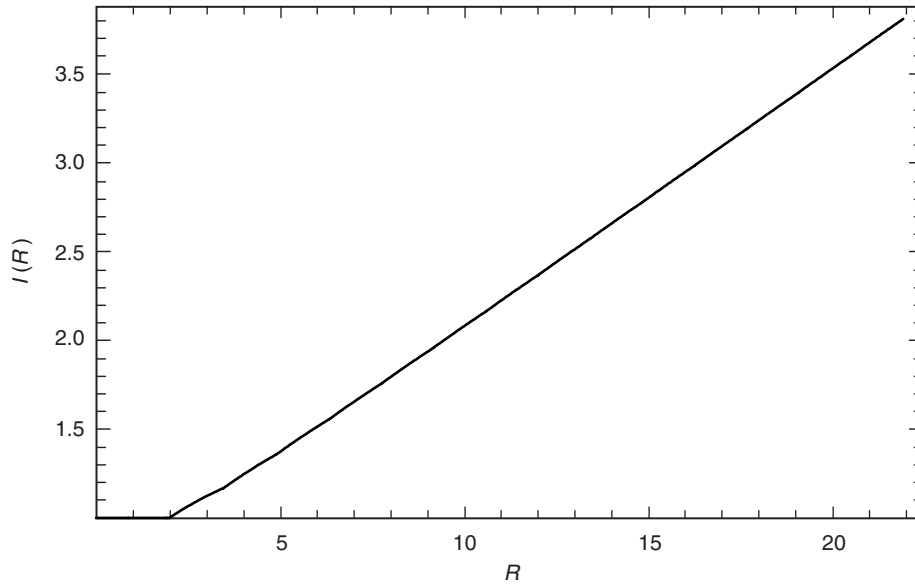

Fig. 6-8. Performance improvement as a function of SNR.

of R, the derivative of $I(R)$ with respect to R is discontinuous at the critical values of R, namely, $R = R_L^+$ for $L \in \{1, 2, 3, \cdots\}$, but the discontinuity becomes monotonically smaller as L increases.

It is also instructive to compare the performance of the optimized realizable estimator $\hat{R}_*$ with that of the fictitious estimator $\hat{R}_\bullet$. The corresponding variance ratio is computed directly from Eq. (6-66), as long as we are careful to delineate the range of validity from Eq. (6-68), where each integer value of L contributes to the optimized estimator $\hat{R}_*$:

$$\frac{\operatorname{var}\left\{\hat{R}_*\right\}}{\operatorname{var}\left\{\hat{R}_\bullet\right\}} = \frac{2/r + 4 + r}{4 + 2\sqrt{2}}, \quad \sqrt{1 - 1/L_*(R)} \leq \frac{r}{\sqrt{2}} \leq \sqrt{1 + 1/L_*(R)} \quad (6\text{-}70)$$

where for the optimized realizable estimator $\hat{R}_*$ the short symbol SNR r is evaluated explicitly in terms of R as $r = R/L_*(R)$. We see that for any value of R the corresponding interval of validity in Eq. (6-70) always includes the optimal point $r = \sqrt{2}$, at which the ratio of variances is unity. Furthermore, since the width of these intervals (measured in terms of r) shrinks to zero as $L_*(R) \to \infty$, the ratio of variances makes smaller and smaller excursions from its value of unity at $r = \sqrt{2}$ as $R \to \infty$, implying $L_*(R) \to \infty$ from Eq. (6-68). Thus, the asymptotic performance for large R and large N of the optimized realizable estimator $\hat{R}_*$ is the same as that of the fictitious estimator $\hat{R}_\bullet$ given in Eq. (6-65). In particular, we see from Eq. (6-65) that $\operatorname{var}\{\hat{R}_*\}$ grows only linearly in the limit of large R, whereas $\operatorname{var}\{\hat{R}_L\}$ for any fixed L eventually grows quadratically for large enough R/L.

As can be seen from Eq. (6-63), the generalized SSME $\hat{R}_L$ is asymptotically unbiased (in the limit as $N \to \infty$). As shown in [6], it is possible to completely remove the bias of the conventional SSME $\hat{R}$ and to define a perfectly unbiased estimator as $\hat{R}^o = \hat{R} - (\hat{R} + 1)/N$. Similarly, we can now define a precisely unbiased version $\hat{R}_L^o$ of our generalized estimator $\hat{R}_L$ by

$$\hat{R}_L^o = \hat{R}_L - \frac{\hat{R}_L + L}{LN} \quad (6\text{-}71)$$

Again we note that the original unbiased SSME $\hat{R}^o$ is just a special case of our generalized unbiased SSME, $\hat{R}^o = \hat{R}_1^o$. Using the definition of Eq. (6-71) together with the expressions in Eq. (6-62) for the exact mean and variance of $\hat{R}_L$, we find that the exact mean and variance of the unbiased estimator $\hat{R}_L^o$ are given by

$$E\left\{\hat{R}_L^o\right\} = R$$

$$\text{var}\left\{\hat{R}_L^o\right\} = \frac{L^2}{LN-2}\left[\left(1+\frac{4R}{L}\right)\left(\frac{LN-1/2}{LN}\right)+\left(\frac{R}{L}\right)^2\right] \tag{6-72}$$

For large N, the asymptotic variance expression obtained from Eq. (6-72) is identical to that already shown in Eq. (6-63) for the biased estimator. Thus, all of the preceding conclusions about the optimal choice of L for a given R, and the resulting optimal estimator performance, apply equally to the unbiased versions $\hat{R}_L^o$ of the estimators $\hat{R}_L$.

6.7 A Method for Improving the Robustness of the Generalized SSME

For any fixed L, our generalized SSME $\hat{R}_L$ is only optimal when the true SNR R lies in the range $\sqrt{2L(L-1)} \leq R \leq \sqrt{2L(L+1)}$. Indeed $\hat{R}_L$ for any $L > 1$ is inferior to the original SSME $\hat{R}_1$ for small enough R (at least for $0 \leq R \leq 2$). The range of optimality for a given value of L, measured in decibels, is just $10\log_{10}\left[\sqrt{2L(L+1)}/\sqrt{2L(L-1)}\right] = 5\log_{10}\left[(L+1)/(L-1)\right]$ dB, which diminishes rapidly toward 0 dB with increasing L. In order to achieve the exact performance of the optimized estimator $\hat{R}_*$ over an unknown range of values of the true SNR R, one would need to select, and then implement, the optimal symbol subdivision based on arbitrarily precise knowledge (measured in decibels) of the very parameter being estimated! Fortunately, there is a more robust version of the generalized SSME that achieves nearly the same performance as $\hat{R}_*$, yet requires only very coarse knowledge about the true SNR R.

To define the robust generalized SSME, we use the same set of estimators $\left\{\hat{R}_L\right\}$ as defined before for any fixed integers L, but now we restrict the allowable choices of L to the set of integers $\{b^\ell, \ell = 0, 1, 2, \cdots\}$, for some integer base $b \geq 2$. The optimal choice of L restricted to this set is denoted by $L_{b*}(R)$, and the corresponding optimized estimator is denoted by $\hat{R}_{b*}$. Because our various estimators differ only in the amount of freedom allowed for the choice of L, their performances are obviously related as

$$\text{var}\left\{\hat{R}_\bullet\right\} \leq \text{var}\left\{\hat{R}_*\right\} \leq \text{var}\left\{\hat{R}_{b*}\right\} \leq \text{var}\left\{\hat{R}_1\right\} \tag{6-73}$$

In this section, we will show analytically that the variance achieved by the robust estimator $\hat{R}_{b*}$ with $b = 2$ comes very close to that achieved by the fictitious estimator $\hat{R}_\bullet$ for all $R \geq 2$, and hence Eq. (6-73) implies that for this range

of R it must be even closer to the less analytically tractable variance achieved by the optimized realizable estimator $\hat{R}_*$. Conversely, for all $R \leq 2$, we have already seen that the optimized realizable estimator $\hat{R}_*$ is the same as the original SSME $\hat{R}_1$, and hence so is the optimized robust estimator $\hat{R}_{b*}$ for any b, since $L = b^0 = 1$ is a permissible value for the robust estimator as well.

The convexity of the general asymptotic variance expression in Eq. (6-63) again allows us to test the optimality of $\hat{R}_{b\ell}$ by simply comparing its performance versus that of its nearest permissible neighbors, $\hat{R}_{b\ell-1}$ and $\hat{R}_{b\ell+1}$. The lower and upper endpoints of the region of optimality for any particular $\hat{R}_{b\ell}$ are determined by equating $\mathrm{var}\{\hat{R}_{b\ell}\}$ with $\mathrm{var}\{\hat{R}_{b\ell-1}\}$ and $\mathrm{var}\{\hat{R}_{b\ell+1}\}$, respectively. This leads to the following definition of the optimal $L_{b*}(R)$ for L restricted to the set $\{b^\ell, \ell = 0, 1, 2, \cdots\}$:

$$
L_{b*}(R) = \begin{cases} b^\ell, & \text{if } \sqrt{2b^{2\ell-1}} \leq R \leq \sqrt{2b^{2\ell+1}} \text{ for integer } \ell \geq 1 \\ b^0 = 1, & \text{if } 0 \leq R \leq \sqrt{2b} \end{cases} \qquad (6\text{-}74)
$$

For all $R \leq \sqrt{2b}$, the optimized estimator $\hat{R}_{b*}$ is the same as the original SSME $\hat{R}_1$. For all $R \geq \sqrt{2/b}$ (which includes the upper portion of the interval over which $l = 0$ is optimum), the variance achieved by $\hat{R}_{b*}$, normalized to that of the fictitious estimator $\hat{R}_\bullet$, is obtained from Eqs. (6-66) and (6-74) in terms of $r = R/L_{b*}(R)$, and upper bounded by

$$
\frac{\mathrm{var}\{\hat{R}_{b*}\}}{\mathrm{var}\{\hat{R}_\bullet\}} = \frac{2/r + 4 + r}{4 + 2\sqrt{2}} \leq \frac{4 + \sqrt{2}\left(\sqrt{b} + 1/\sqrt{b}\right)}{4 + 2\sqrt{2}}, \quad \frac{1}{\sqrt{b}} \leq \frac{r}{\sqrt{2}} \leq \sqrt{b} \quad (6\text{-}75)
$$

As with the earlier expression of Eq. (6-70) for the variance of $\hat{R}_*$, the intervals of validity in Eq. (6-75) for any value of R always include the optimal point $r = \sqrt{2}$ at which the ratio of variances is unity. But unlike Eq. (6-70), the width of the intervals in Eq. (6-75) stays constant independently of r. The upper limit on the variance ratio shown in Eq. (6-75) occurs at the end points of these intervals, i.e., for SNR values expressible as $R = \sqrt{2b^{2\ell-1}}$ for some integer $\ell \geq 0$. This upper limit is the maximum excursion from unity of the variance ratio for all $R \geq \sqrt{2/b}$. For all $R \leq 2$ and any $b \geq 2$, there is no limit on the suboptimality of $\hat{R}_{b*}$ with respect to the fictitious estimator $\hat{R}_\bullet$, but in this range $\hat{R}_{b*}$ suffers no suboptimality with respect to the optimized realizable estimator $\hat{R}_*$, since

both are equivalent to the original SSME $\hat{R}_1$ for $R \leq 2$. Finally, reiterating our earlier conclusion based on the simple inequalities in Eq. (6-73), we conclude that the maximum degradation $D(R)$ of the robust estimator $\hat{R}_{b*}$ with respect to the optimized realizable estimator $\hat{R}_*$ is upper bounded for all R by

$$D(R) = \frac{\text{var}\left\{\hat{R}_{b*}\right\}}{\text{var}\left\{\hat{R}_*\right\}} \leq \frac{\text{var}\left\{\hat{R}_{b*}\right\}}{\text{var}\left\{\hat{R}_\bullet\right\}} \leq \frac{4 + \sqrt{2}\left(\sqrt{b} + 1/\sqrt{b}\right)}{4 + 2\sqrt{2}} \quad \text{for all } R \quad (6\text{-}76)$$

For example, we consider the case of $b = 2$, which yields permissible values of L given by $L = 1, 2, 4, 8, 16, \cdots$ and corresponding decision region boundaries at $R = 1, 2, 4, 8, 16, \cdots$, i.e., regions separated by 3 dB. From Eq. (6-76), the maximum degradation $D_{\max}$ for using the coarsely optimized estimator $\hat{R}_{2*}$ instead of the fully optimized realizable estimator $\hat{R}_*$ is no more than

$$D_{\max} \leq \frac{7}{4 + 2\sqrt{2}} = 1.02513 \tag{6-77}$$

i.e., a penalty of only 2.5 percent. Even if we were to enlarge the regions of constant $L_{b*}(R)$ to a width of 9 dB in R (corresponding to $b = 8$), the maximum penalty would increase only to

$$D_{\max} \leq \frac{8.5}{4 + 2\sqrt{2}} = 1.245 \tag{6-78}$$

i.e., a penalty just under 25 percent. Thus, even though the optimized generalized SSME $\hat{R}_*$ requires (in principle) very precise prior knowledge of the true value of R, its performance can be reasonably well approximated by that of a robust estimator $\hat{R}_{b*}$ requiring only a very coarse prior estimate of R.

6.8 Special Case of the SSME for BPSK-Modulated Data

We can define an analogous sequence of generalized SSMEs $\{\tilde{R}_L, L = 1, 2, \cdots\}$ corresponding to the original SSME $\tilde{R} = \tilde{R}_1$ developed for BPSK signals using real-valued in-phase samples only. In this case, the (exact) mean and variance of the original SSME $\tilde{R}$ are given by [4]

$$E\left\{\tilde{R}\right\} = R + \frac{2R+1}{N-2}$$

$$\text{var}\left\{\tilde{R}\right\} = \frac{1}{N-4}\left(\frac{N}{N-2}\right)^2\left[(1+4R)\left(\frac{N-1}{N}\right)+2R^2\right]$$

$$(6\text{-}79)$$

The mean and variance of the generalized SSME $\tilde{R}_L$ based on real-valued samples are obtained from Eq. (6-79) by following the same reasoning that led to Eq. (6-62):

$$E\left\{\tilde{R}_L\right\} = L\left[\frac{R}{L}+\frac{2R/L+1}{LN-2}\right] = R + \frac{2R+L}{LN-2}$$

$$\text{var}\left\{\tilde{R}_L\right\} = \frac{L^2}{LN-4}\left(\frac{LN}{LN-2}\right)^2\left[\left(1+\frac{4R}{L}\right)\left(\frac{LN-1}{LN}\right)+2\left(\frac{R}{L}\right)^2\right]$$

$$(6\text{-}80)$$

and the asymptotic forms for large N, i.e., $N \gg 1$, are within $O(1/N^2)$ of

$$E\left\{\tilde{R}_L\right\} = R + \frac{2R+L}{LN}$$

$$\text{var}\left\{\tilde{R}_L\right\} = \frac{L}{N}\left[1+4\left(\frac{R}{L}\right)+2\left(\frac{R}{L}\right)^2\right]$$

$$(6\text{-}81)$$

We can argue as in [5] that the first- and second-order statistics of the SSME $\hat{R}_L$ based on complex samples are derivable from those of the SSME $\tilde{R}_L$ based on real samples. Specifically, since $\hat{R}_L$ is obtained from twice as many real observables as $\tilde{R}_L$, with (on average) only half the SNR (since the SNR is zero in the quadrature component for BPSK signals), we have the following (exact) equalities:

$$E\left\{\frac{\hat{R}_L}{2}\right\}\Big|_{(R,N)} = E\left\{\tilde{R}_L\right\}\Big|_{([R/2],2N)}$$

$$\text{var}\left\{\frac{\hat{R}_L}{2}\right\}\Big|_{(R,N)} = \text{var}\left\{\tilde{R}_L\right\}\Big|_{([R/2],2N)}$$

$$(6\text{-}82)$$

where now we have explicitly denoted the dependence of $\hat{R}_L$ and $\tilde{R}_L$ on the SNR and the number of symbols. The equalities in Eq. (6-82) can be verified by direct comparison of Eq. (6-80) with Eq. (6-62) and Eq. (6-81) with Eq. (6-63).

As in our earlier analysis of the generalized SSME $\hat{R}_L$ based on complex-valued samples, we can also optimize the generalized SSME $\tilde{R}_L$ based on real-valued samples with respect to its asymptotic performance expressions in Eq. (6-81). We define for any fixed value of R an optimum integer $L = \tilde{L}_*(R)$ and an optimum real number $L = \tilde{L}_\bullet(R)$ to minimize the asymptotic variance expression in Eq. (6-81), and corresponding optimal realizable and fictitious estimators $\tilde{R}_*$ and $\tilde{R}_\bullet$. For the optimum realizable estimate, we find, corresponding to Eq. (6-68), that the optimum integer $\tilde{L}_*(R)$ is evaluated as

$$\tilde{L}_*(R) = L, \quad \text{if} \quad \sqrt{L\left(L-1\right)/2} \le R \le \sqrt{L\left(L+1\right)/2} \qquad (6\text{-}83)$$

We find, corresponding to Eqs. (6-64) and (6-65), that the optimal real value of L is $\tilde{L}_\bullet(R) = R\sqrt{2}$ and the corresponding variance is

$$\mathrm{var}\left\{\tilde{R}_\bullet\right\} = \frac{R}{N}\left(4 + 2\sqrt{2}\right) = \mathrm{var}\left\{\hat{R}_\bullet\right\} \qquad (6\text{-}84)$$

In other words, the fictitious estimator achieves identical variance using either real samples or complex samples.

Finally, we observe from a comparison of Eqs. (6-62) and (6-80) an interesting (exact) relationship between the means and variances of the two generalized SSMEs for different values of the symbol rate oversampling factor L:

$$E\left\{\hat{R}_L\right\} = E\left\{\tilde{R}_{2L}\right\}$$

$$\mathrm{var}\left\{\hat{R}_L\right\} = \mathrm{var}\left\{\tilde{R}_{2L}\right\}$$

$$(6\text{-}85)$$

Thus, the estimators $\tilde{R}_L$ based on real samples can be viewed as a more finely quantized sequence than the estimators $\hat{R}_L$ based on complex samples, in that any mean and variance achievable by an estimator in the latter sequence is also achievable by taking twice as many subintervals in a corresponding estimator from the former sequence. This implies, for example, that the maximum deviation of the variances of $\tilde{R}_*$ and $\tilde{R}_\bullet$ is no greater than that calculated in Eq. (6-70) for the deviation between the variances of $\hat{R}_*$ and $\hat{R}_\bullet$.

6.9 Comparison with the Cramer–Rao Lower Bound on the Variance of SNR Estimators

A good benchmark for the performance of a given SNR estimator is the Cramer–Rao (C-R) lower bound on its variance [11]. Here we present for comparison the C-R lower bound for any SNR estimator using a given number of observables (samples) per symbol interval, with or without knowledge of the data. For simplicity, we consider only estimators based on real observables, since a number of C-R bounds reported elsewhere [1,12,13] have explicitly considered that case.

It has been shown in [13] that the C-R lower bound on the variance of an arbitrary unbiased estimator of SNR, R^*, in the presence of unknown binary equiprobable data and K independent real observations per symbol (K subinterval samples) is given by

$$\text{var}\{R^*\} \geq \frac{2R^2}{N}\left[\frac{2K + 2R - E_2(2R)}{2KR - (4R + K)E_2(2R)}\right] \qquad (6\text{-}86)$$

where

$$E_2(2R) = E\left\{X^2\text{sech}^2 X\right\} \qquad (6\text{-}87)$$

with X a Gaussian random variable with mean and variance both equal to $2R$. The expectation in Eq. (6-87), which depends only on R, cannot be determined in closed form but is easily evaluated numerically. Figure 6-9, described at the end of this section, compares the C-R bounding variance in Eq. (6-86) with the actual asymptotic variance in Eq. (6-81) achieved by the generalized SSME $\tilde{R}_L$ based on real samples. For this comparison, we substitute $K = 2L$ in the C-R bound expression (because there are $K = 2L$ subinterval integrations contributing to the SSME $\tilde{R}_L$), and we plot the cases $L = 1, 2, 4, \infty$.

We can also perform analytic comparisons in the limits of low and high SNR. The low- and high-SNR behavior of the C-R bounding variance in Eq. (6-86) is given by [13]

$$\text{var}\{R^*\} \geq \begin{cases} \dfrac{1}{2N}\left(\dfrac{K}{K-1}\right), & R \ll 1 < K \\[3mm] \dfrac{2R}{N}\left(1 + \dfrac{R}{K}\right), & R \gg K \end{cases} \qquad (6\text{-}88)$$
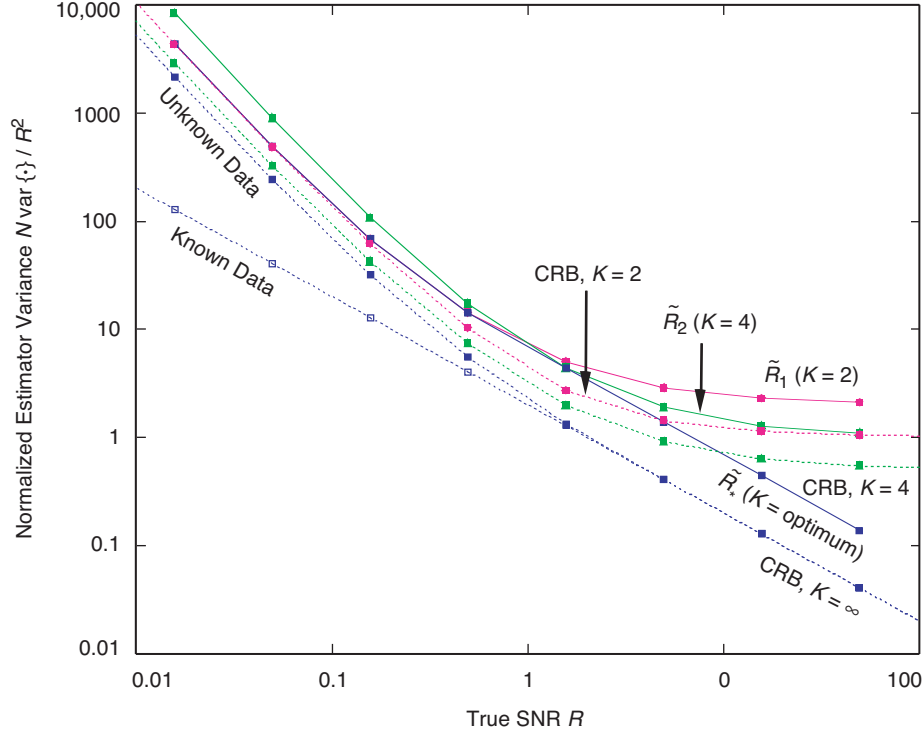
Fig. 6-9. A comparison of the performance of several SNR estimators with the Cramer–Rao bound.

By comparison, the asymptotic expression in Eq. (6-81) for the variance of $\tilde{R}_L$ for any fixed L reduces in the low- and high-SNR limits to

$$
\operatorname{var}\left\{\tilde{R}_L\right\} \cong
\begin{cases}
\dfrac{L}{N} = \dfrac{K}{2N}, & L \gg R \\[3mm]
\dfrac{2R^2}{NL}\left(1 + \dfrac{2L}{R}\right) = \dfrac{4R}{N}\left(1 + \dfrac{R}{K}\right), & R \gg L
\end{cases}
\tag{6-89}
$$

Compared to the C-R bounding variance in Eq. (6-88), the actual variance in Eq. (6-89) is higher by a factor of $K - 1$ in the low-SNR limit and by a factor of two in the high-SNR limit.

For any fixed K, the C-R bounding variance in Eq. (6-86) becomes quadratic in R as R approaches infinity, as evidenced by the second expression in Eq. (6-89). On the other hand, the limiting behavior of the bound for K approaching infinity with fixed R is given by

$$\operatorname{var}\left\{R^*\right\} \geq \frac{1}{N}\left[\frac{4R^2}{2R - E_2\left(2R\right)}\right], \quad K \gg \max\left(R, 1\right) \tag{6-90}$$

Since $E_2(2R) = 2R + 8R^2 + O\left(R^3\right)$ for small R and is exponentially small for large R [13], the C-R bounding variance on the right side of Eq. (6-90) approaches a constant at low SNR and becomes linear in R at high SNR:

$$\operatorname{var}\left\{R^*\right\} \geq \begin{cases} \dfrac{1}{2N}, & K \gg 1 \gg R \\[2mm] \dfrac{2R}{N}, & K \gg R \gg 1 \end{cases} \tag{6-91}$$

Since the C-R bounding expressions in Eqs. (6-90) and (6-91) for large values of $K = 2L$ reflect the best possible performance of an estimator with access to a continuum of samples within each symbol, they are suitably compared to the performance of the optimized estimator $\tilde{R}_*$, rather than to the performance of $\tilde{R}_L$ for any fixed L. As an approximation to $\tilde{R}_*$, we use a stand-in estimator equal to $\tilde{R}_1$ for $R \leq 2$ (i.e., where $\tilde{L}_*(R) = 1$) and to the fictitiously optimized estimator $\tilde{R}_\bullet$ for $R > 2$. The corresponding asymptotic variances computed from Eq. (6-81) for the limits corresponding to those in Eq. (6-91) are

$$\begin{cases} \operatorname{var}\left\{\tilde{R}_1\right\} = \dfrac{1}{N}, & 1 \gg R \\[2mm] \operatorname{var}\left\{\tilde{R}_\bullet\right\} = \dfrac{R}{N}\left(4 + 2\sqrt{2}\right), & R \gg 1 \end{cases} \tag{6-92}$$

The estimator variances in Eq. (6-92) are higher than the corresponding C-R bounding variances in Eq. (6-91) by a factor of 2 in the low-SNR limit and by a factor of $2 + \sqrt{2} \cong 3.4$ in the high-SNR limit. The optimized *realizable* estimator $\tilde{R}_*$ suffers an additional small suboptimality factor with respect to the performance of the fictitious estimator $\tilde{R}_\bullet$ used as its stand-in in Eq. (6-92).

Finally we consider for purposes of comparison the C-R bound on an arbitrary unbiased estimator when the data are perfectly known. The C-R bound under this assumption is well known, e.g., [11]. Here we continue with the notation of [13] by noting that the derivation there for the case of unknown data is easily modified to the known data case by skipping the average over the binary equiprobable data. The result is equivalent to replacing the function $E_2\left(2R\right)$ by zero in the C-R bound expression in Eq. (6-41), i.e.,

$$\operatorname{var}\left\{\hat{R}\right\} \geq \frac{2R^2}{N}\left[\frac{2K + 2R}{2KR}\right] = \frac{2R}{N}\left(1 + \frac{R}{K}\right), \quad \text{for all } K, R \tag{6-93}$$

We compare this bound for known data, which is valid for all K and R, with the high-SNR bound for unknown data given by the second expression in Eq. (6-88), which is valid for any fixed K as $R \to \infty$. These two variance expressions are identical because the second expression in Eq. (6-88) was obtained from Eq. (6-86) using the approximation that $E_2(2R)$ is exponentially small for large R. Thus, we reach the interesting and important conclusion that, based on the C-R bounds, *knowledge of the data is inconsequential in improving the accuracy of an optimized SNR estimator at high enough SNR*! We also note that the limiting fractional variance, $\text{var}\{R^*\}/(R^*)^2$, in either case is simply $2/(NK)$, i.e., it falls in proportion to the total number NK of samples collected. In this limit, therefore, it does not matter to an optimal estimator whether it collects the same total number of samples in step with the symbol rate or faster. From the second expression in Eq. (6-89), we see that our generalized SSME $\tilde{R}_L$ behaves similarly to an optimum estimator in this respect, because the ratio of its fractional variance to the C-R bounding variance is a constant factor of 2 when $R \gg K$. Whereas with the original SSME one might need to wait N_{req} symbol periods to reach a desired estimator variance, our generalized SSME now offers the capability at high enough SNR to reach this same variance within N_{req}/L symbol periods. Since any practical system will impose limits on the integrate-and-dump rate, and hence on L, this waiting time for acceptable estimator variance cannot be made arbitrarily small. However, at high SNR our generalized SSME allows this waiting time to be reduced down to the limits arising from the system's sampling rate if so desired.

At low SNR, we have seen from the first expression in Eq. (6-88) that the C-R bounding variance (not the fractional variance) for the case of unknown data hits a nonzero floor at $(1/2N)K/(K-1)$ no matter how closely R approaches zero, whereas the bounding variance in Eq. (6-93) for the case of known data goes to zero linearly in R. Thus, knowledge of the data fundamentally changes the behavior of the C-R bound at low SNR, and it can be quite helpful in this region for improving the accuracy of the estimator. Inspection of Eqs. (6-93) and (6-88) in the limit of small R shows that, in contrast to the case for high SNR, oversampling confers no benefit (with known data) or virtually no benefit (with unknown data) to the performance of an optimized estimator at low SNR. Indeed, we see from Eq. (6-89) that the performance of our generalized SSME in this limit is actually worsened by oversampling. Thus, the waiting time to achieve acceptable estimator variance at low SNR is dictated by the symbol rate, even if the system's sampling rate capabilities are significantly faster.

Figure 6-9 summarizes the comparisons of our generalized SSME with the relevant C-R bounds (CRB). This figure plots the CRB as a function of true SNR R, for $K = 2, 4, \infty$ with unknown data, and for $K = \infty$ with known data.

Also shown for comparison are the actual asymptotic variances achieved by the original SSME $\tilde{R}_1$, the generalized SSME $\tilde{R}_2$ using four subinterval integrations within each symbol, and the optimized generalized SSME $\tilde{R}_*$. In each case, the asymptotic variance is plotted in normalized form as $N\text{var}\{\cdot\}/R^2$, which can be interpreted as the number of symbols N that must be observed to achieve a *fractional* estimator variance of 100 percent; smaller fractional variances require inversely proportionately larger numbers of symbols. Also, since asymptotically for large N, $\text{var}\{\cdot\}/R^2$ is an inverse measure of the "quality" of the estimator as previously defined, which for large R varied inversely with N, then asymptotically for large R, $N\text{var}\{\cdot\}/R^2$ is an inverse measure of this quality with the dependence on observation time normalized out.

6.10 Improvement in the Presence of Frequency Uncertainty

Earlier in the chapter and in [6] we considered the performance of the conventional ($L = 1$) SSME in the presence of carrier phase and frequency uncertainties for a variety of cases corresponding to the degree to which the frequency uncertainty is estimated and compensated for. Here we extend these results to the generalized SSME, i.e., we examine the improvement in performance when frequency uncertainty is present, obtained by optimally partitioning the symbol interval in accordance with the value of the true SNR. In the case where the frequency uncertainty is not estimated, one has no choice other than to use the SNR boundaries determined in the no-frequency-uncertainty case, i.e., those given in Eq. (6-68) or Eq. (6-74). For the cases where an estimate of the frequency uncertainty is available, and therefore can be compensated for, one can use this information, if desired, to modify the SNR boundaries. However, to a first-order approximation, we shall assume in what follows that we always determine the boundaries for the symbol regions of fixed partitioning from their zero-frequency uncertainty values. This allows one to implement a fixed-SSME configuration independent of the knowledge of the frequency error and yet still to obtain the possibility of a performance advantage relative to the conventional half-symbol split structure. To illustrate the application of the principles involved and resulting performance gains obtained, we shall consider only a few of the cases previously treated.

●**Case 1: Frequency Uncertainty, No Frequency Estimation (and thus No Phase Compensation)**

For this case, it was shown earlier that the variance of the conventional SSME is given by Eq. (6-26). To modify this expression for the case of $2L$ partitions

of the symbol interval, we proceed as before by replacing R by R/L, N by LN, δ by δ/L, and then multiplying the result by L^2, resulting in[5]

$$\mathrm{var}\left\{\hat{R}_L\right\} =$$

$$L^2 \left(\frac{LN}{LN-1}\right)^2 \left\{\left(\frac{LN-1}{LN-2}\right)\left[\frac{\left(1+2h^+\left(\frac{\delta}{L}\right)\frac{R}{L}\right)}{LN}+\left(1+h^+\left(\frac{\delta}{L}\right)\frac{R}{L}\right)^2\right]\right.$$

$$\times\ {}_1F_1\left(2;LN;-Nh^-\left(\frac{\delta}{L}\right)R\right)-\left(1+h^+\left(\frac{\delta}{L}\right)\frac{R}{L}\right)^2$$

$$\times\ \left.\left[{}_1F_1\left(1;LN;-Nh^-\left(\frac{\delta}{L}\right)R\right)\right]^2\right\} \tag{6-94}$$

Then, the improvement in performance is obtained by taking the ratio of Eq. (6-26) to Eq. (6-94), i.e.,

$$I\left(R\right) = \frac{\mathrm{var}\left\{\hat{R}\right\}}{\mathrm{var}\left\{\hat{R}_L\right\}} \tag{6-95}$$

where, for a value of R in the interval $R_L^- \leq R < R_L^+$, the value of L to be used corresponds to that determined from Eq. (6-68) or alternatively from Eq. (6-74). We note that since the boundaries of the SNR regions of Eqs. (6-68) and (6-74) are determined from the asymptotic (large N) expressions for the estimator variance, a plot of $I(R)$ versus R determined from Eq. (6-95) will exhibit small discontinuities at these boundaries. These discontinuities will become vanishingly small as N increases.

Figures 6-10 and 6-11 illustrate such a plot for values of N equal to 20 and 100, respectively, with δ as a parameter. We make the interesting observation that, although on an absolute basis the variance of the estimator monotonically improves with increasing N, the improvement factor as evaluated from Eq. (6-95), which makes use of the exact expression for the estimator variance, shows a larger improvement for smaller values of N. To see how this comes about analytically,

---

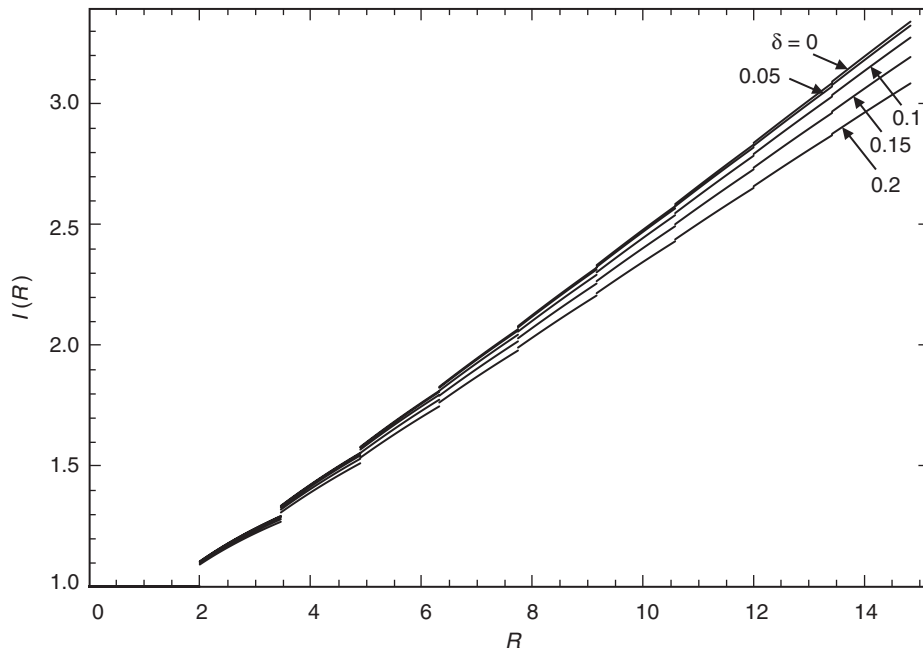[5] To make matters clear, we now include the dependence of $h^\pm$ on δ in the notation.

Fig. 6-10. Improvement factor versus SNR with normalized frequency uncertainty as a parameter; Case 1; $N = 20$.
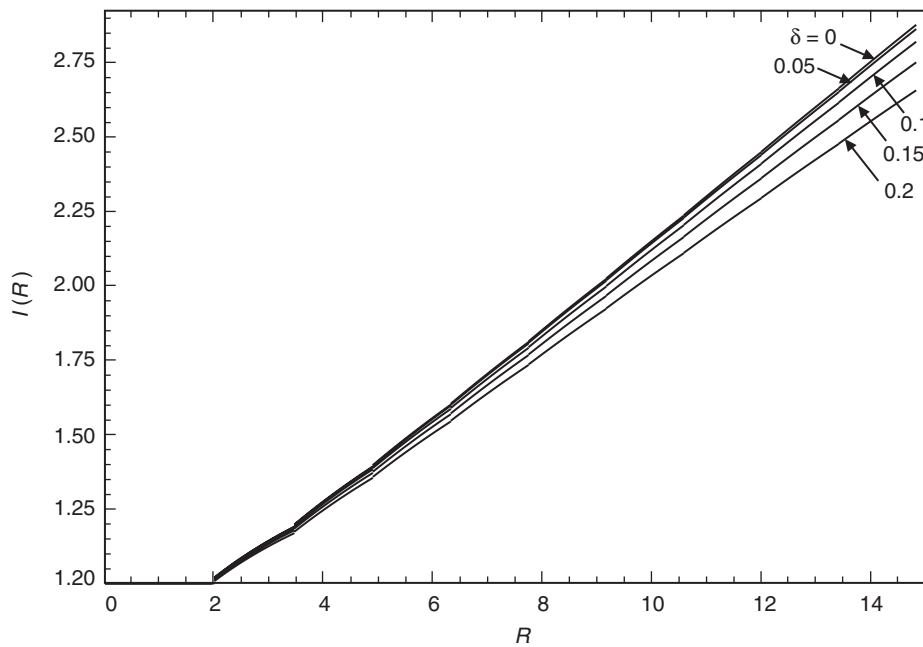

Fig. 6-11. Improvement factor versus SNR with normalized frequency uncertainty as a parameter; Case 1; $N = 100$.

we examine the behavior of the zero-frequency uncertainty improvement factor for large SNR. For sufficiently large SNR (equivalently, large L), we obtain from Eq. (6-62) the same asymptotic expression as given in Eq. (6-63) when assuming N large. Also, since for large SNR L and R are approximately related by $L = R/\sqrt{2}$, then substituting this in Eq. (6-63) gives the asymptotic result

$$\mathrm{var}\left\{\hat{R}_L\right\} \cong \frac{R}{N}\left(4 + 2\sqrt{2}\right) \tag{6-96}$$

From Eq. (6-61), we have for sufficiently large SNR

$$\mathrm{var}\left\{\hat{R}\right\} = \frac{1}{N-2}\left(\frac{N}{N-1}\right)^2 R^2 \tag{6-97}$$

Thus, the improvement factor for large SNR is the ratio of Eq. (6-97) to Eq. (6-96), namely,

$$I(R) = \frac{\dfrac{1}{N-2}\left(\dfrac{N}{N-1}\right)^2 R^2}{\dfrac{R}{N}\left(4 + 2\sqrt{2}\right)} = \frac{R}{4 + 2\sqrt{2}}\left(\frac{N}{N-2}\right)\left(\frac{N}{N-1}\right)^2 \tag{6-98}$$

which, for a given R, is a monotonically decreasing function of N approaching $I(R) = R/\left(4 + 2\sqrt{2}\right)$ in the limit as $N \to \infty$.

•Case 2b: Frequency Uncertainty, Perfect Frequency Estimation, Fractional-Symbol Phase Compensation

The case where the frequency uncertainty is perfectly estimated and then used to compensate for the phase shift caused by this uncertainty in the second half of the symbol interval variance of the estimator was given in Eq. (6-30). Making the same substitutions as before, for a $2L$-partition of the symbol interval we obtain

$$\mathrm{var}\left\{\hat{R}_L\right\} =$$

$$L^2 \frac{1}{(h^+\,(\delta/L))^2} \frac{1}{LN - 2}\left(\frac{LN}{LN - 1}\right)^2 \left[\left(1 + 2h^+\left(\frac{\delta}{L}\right)\frac{R}{L}\right)\left(\frac{2LN - 1}{LN}\right)\right.$$

$$\left. + \left(h^+\left(\frac{\delta}{L}\right)\frac{R}{L}\right)^2\right] \tag{6-99}$$

Comparing Eq. (6-30) with Eq. (6-61), we observe that, in this case, the variance of $h^+(\delta)\,\hat{R}$ for the conventional SSME is identical to the variance of $\hat{R}$ in the zero-frequency uncertainty case. From a comparison of Eqs. (6-99) and (6-62), a similar equivalence can be made between the variance of $h^+(\delta/L)\,\hat{R}$ and the variance of $\hat{R}$ for the $2L$-partition estimator.

Analogous to what was done for Case 1, the improvement factor, $I(R)$, here can be obtained from the ratio of Eq. (6-30) to Eq. (6-99). Figures 6-12 and 6-13 are plots of $I(R)$ versus true SNR, R, for values of N equal to 20 and 100, respectively, with δ as a parameter. Once again we make the observation that a larger improvement is obtained for smaller values of N. An analytical justification for this observation can be demonstrated by examining the behavior of I for large SNR. Specifically, the analogous expression to Eq. (6-98) now becomes

$$I(R) = \frac{\left(\dfrac{1}{(h^+(\delta))^2\,R} + \dfrac{2}{h^+(\delta)}\right)\left(\dfrac{2N-1}{N}\right) + R}{\dfrac{4}{h^+\left(\sqrt{2}\delta/R\right)} + \sqrt{2}\left(1 + \dfrac{1}{\left(h^+\left(\sqrt{2}\delta/R\right)\right)^2}\right)} \left(\frac{N}{N-2}\right)\left(\frac{N}{N-1}\right)^2$$

$$(6\text{-}100)$$

which for sufficiently large R relative to δ (i.e., $h^+\left(\sqrt{2}\delta/R\right) \cong 1$) becomes

$$I(R) = \frac{\left(\dfrac{1}{(h^+(\delta))^2\,R} + \dfrac{2}{h^+(\delta)}\right)\left(\dfrac{2N-1}{N}\right) + R}{4 + 2\sqrt{2}} \left(\frac{N}{N-2}\right)\left(\frac{N}{N-1}\right)^2$$

$$(6\text{-}101)$$

Once again we see in Figs. 6-12 and 6-13 the same dependence on N as before approaching

$$I(R) = \frac{2\left(\dfrac{1}{(h^+(\delta))^2\,R} + \dfrac{2}{h^+(\delta)}\right) + R}{4 + 2\sqrt{2}} \qquad (6\text{-}102)$$

in the limit as $N \to \infty$. We also note that, whereas in the previous figures for a given value of R the improvement factor decreased with increasing frequency uncertainty, here it increases, which is consistent with Eq. (6-102) since
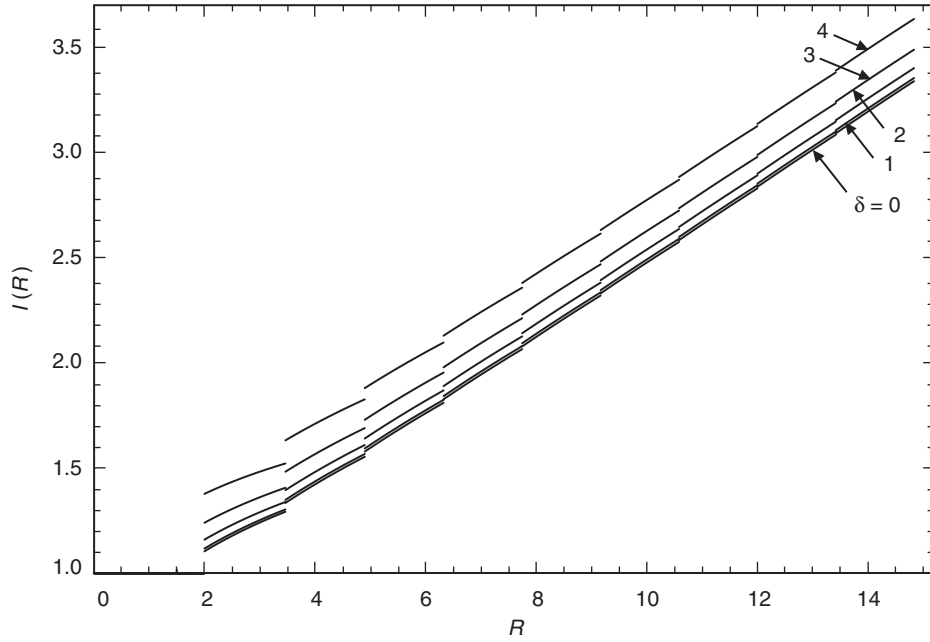
Fig. 6-12. Improvement factor versus SNR with normalized frequency uncertainty as a parameter; Case 2b; $N = 20$.
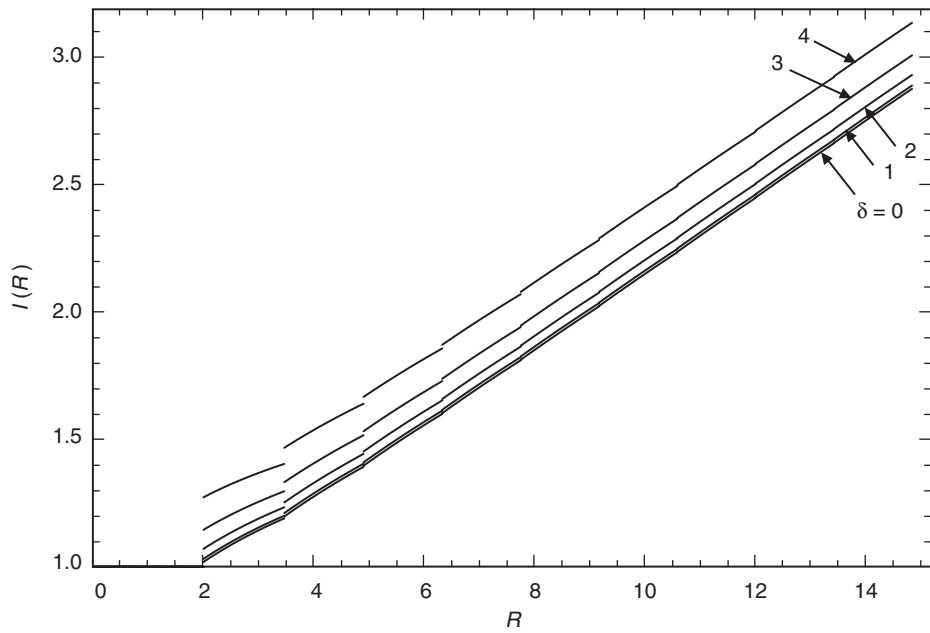

Fig. 6-13. Improvement factor versus SNR with normalized frequency uncertainty as a parameter; Case 2b; $N = 100$.

$h^+ (\delta) = \text{sinc}^2 (\delta/4)$ is a monotonically decreasing function of δ. The intuitive reason for this occurrence is that, for the conventional SSME, the performance degrades much more severely in the presence of large frequency uncertainty than for the improved SSME since for the former the degradation factor $h^+ (\delta)$ operates out on its tail, whereas for the latter the effective frequency uncertainty is reduced by a factor of L, and thus for large L the degradation factor $h^+(\delta/L) \cong h\big(\sqrt{2}\delta/R\big)$ operates near its peak of unity. Eventually, for sufficiently large R, the improvement approaches $I(R) = R/\big(4 + 2\sqrt{2}\big)$ as in Case 1. Finally, comparing Figs. 6-12 and 6-13 with Figs. 6-10 and 6-11, we observe that much larger frequency uncertainties can be tolerated for Case 2b than for Case 1.

6.11 The Impact of the Oversampling Factor on the Performance of the Modified SSME in the Presence of Symbol Timing Error

In Section 6.5 we investigated the performance of the conventional SSME in the presence of symbol timing error. From the results given there, we see for example that if the fractional symbol timing error ε were equal to $1/2$, then from Eqs. (6-49) and (6-51) we would have that

$$E \left\{ U^\pm \right\} = 2\sigma^2 \left(1 + \frac{R}{2} \right) \tag{6-103}$$

in which case the performance of the SSME completely degenerates. Since it is desirable to perform SNR estimation prior to obtaining symbol synchronization, it would be advantageous to reduce the sensitivity of the operation of the SSME to knowledge of the symbol timing offset. As we shall show shortly, interestingly enough this can be accomplished by employing an oversampling factor L greater than unity. In fact, the larger the value of L, the less the sensitivity, and in the limit of sufficiently large L, the SSME performance becomes independent of knowledge of the symbol timing.

To illustrate the above statements, assume that for a given L the fractional symbol timing error ε is quantized to $\varepsilon = L_\varepsilon/L$, where for L even, L_ε can take on any of the integer values $0, 1, 2, \cdots, L/2$, and for L odd, L_ε can take on any of the integer values $0, 1, 2, \cdots, (L-1)/2$. Under these circumstances, in the absence of frequency error, the first and second half-symbol I&D outputs would be given by

$$Y_{akl} = md_k \frac{L}{T} \int_{(k-1+(l-1+L_\epsilon)/L)T}^{(k-1+(l-1/2+L_\epsilon)/L)} e^{j\phi} dt + \frac{L}{T} \int_{(k-1+(l-1+L_\epsilon)/L)T}^{(k-1+(l-1/2+L_\epsilon)/L)} n(t) dt$$

$$= \frac{md_k}{2} e^{j\phi} + n_{akl}$$

$$(6\text{-}104)$$

$$Y_{\beta l} = md_k \frac{L}{T} \int_{(k-1+(l-1/2+L_\epsilon)/L)T}^{(k-1+(l+L_\epsilon)/L)} e^{j\phi} dt + \frac{L}{T} \int_{(k-1+(l-1/2+L_\epsilon)/L)T}^{(k-1+(l+L_\epsilon)/L)} n(t) dt$$

$$= \frac{md_k}{2} e^{j\phi} + n_{\beta kl}, \quad l = 1, 2, \cdots, L - L_e$$

and

$$Y_{akl} = md_{k+1} \frac{L}{T} \int_{(k-1+(l-1+L_\epsilon)/L)T}^{(k-1+(l-1/2+L_\epsilon)/L)} e^{j\phi} dt + \frac{L}{T} \int_{(k-1+(l-1+L_\epsilon)/L)T}^{(k-1+(l-1/2+L_\epsilon)/L)} n(t) dt$$

$$= \frac{md_{k+1}}{2} e^{j\phi} + n_{akl}$$

$$(6\text{-}105)$$

$$Y_{\beta l} = md_{k+1} \frac{L}{T} \int_{(k-1+(l-1/2+L_\epsilon)/L)T}^{(k-1+(l+L_\epsilon)/L)} e^{j\phi} dt + \frac{L}{T} \int_{(k-1+(l-1/2+L_\epsilon)/L)T}^{(k-1+(l+L_\epsilon)/L)} n(t) dt$$

$$= \frac{md_{k+1}}{2} e^{j\phi} + n_{\beta kl}, \quad l = L - L_\epsilon + 1, L - L_\epsilon + 2, \cdots, L$$

where $n_{\alpha kl}$ and $n_{\beta kl}$ are zero-mean Gaussian RVs with variance independent of the value of ε. Thus, in so far as the modified SSME is concerned, the partitioning of each symbol into L pairs of subdivisions occurs as before with, however, the first $L - L_\epsilon$ now containing the data symbol d_k and the remaining L_ε ones containing the data symbol d_{k+1}. However, since the statistics of the SSME are independent of the data symbols themselves, then we conclude that for the assumed quantization of ε, *the performance of the SSME is independent of the value of symbol timing error.*

Next assume that for a given L the fractional symbol timing error ε is quantized to $\varepsilon = (L_\varepsilon + 1/2)/L$, where again for L even, L_ε can take on any of the integer values $0, 1, 2, \cdots, L/2$, and for L odd, L_ε can take on any of the integer values $0, 1, 2, \cdots, (L-1)/2$. Under these circumstances, in the absence of frequency error, the first and second half-symbol I&D outputs would be given by

the results in Eqs. (6-104) and (6-105) for all values of l with the exception of $l = L - L_\varepsilon$, in which case these outputs become

$$Y_{akl}\,|_{l=L-L_\varepsilon} = \frac{md_k}{2}e^{j\phi} + n_{akl}\,|_{l=L-L_\varepsilon}$$

$$\quad (6\text{-}106)$$

$$Y_{\beta l}\,|_{l=L-L_\varepsilon} = \frac{md_{k+1}}{2}e^{j\phi} + n_{\beta kl}\,|_{l=L-L_\varepsilon}$$

In this case, the sum and difference of the first and second half-symbol I&D outputs become

$$u_{kl}^+ = md_k e^{j\phi} + n_{akl} + n_{\beta kl}$$

$$u_{kl}^- = n_{akl} - n_{\beta kl}, \quad l = 1, 2, \cdots, L - L_\varepsilon - 1$$

$$u_{kl}^+\,|_{l=L-L_\varepsilon} = m\left(\frac{d_k + d_{k+1}}{2}\right)e^{j\phi} + n_{akl}\,|_{l=L-L_\varepsilon} + n_{\beta kl}\,|_{l=L-L_\varepsilon}$$

$$\quad (6\text{-}107)$$

$$u_{kl}^-\,|_{l=L-L_\varepsilon} = m\left(\frac{d_k - d_{k+1}}{2}\right)e^{j\phi} + n_{akl}\,|_{l=L-L_\varepsilon} - n_{\beta kl}\,|_{l=L-L_\varepsilon}$$

$$u_{kl}^+ = md_{k+1}e^{j\phi} + n_{akl} + n_{\beta kl}$$

$$u_{kl}^- = n_{akl} - n_{\beta kl}, \quad l = L - L_\varepsilon + 1, L - L_\varepsilon + 2, \cdots, L$$

Thus, for the kth symbol, $L - 1$ sum and difference pairs contribute values whose statistics are independent of the value of ε (and thus the same as in the ideal SSME), whereas one sum and difference pair contributes values whose statistics are different from those of the ideal SSME and thus will result in some degradation of performance. To quantify this performance degradation, we need to compute the statistics of the accumulated squared norms of the sum and difference RVs in Eq. (6-107), namely, $U^\pm = (1/NL)\sum_{k=1}^{N}\sum_{l=1}^{L}\left|u_{kl}^\pm\right|^2$. After some effort, the results for the means and variances, assuming for simplicity BPSK modulation, are as follows:

$$E\left\{U^+\right\} = m^2\left(\frac{L-1/2}{L}\right) + 2\sigma^2 L = 2\sigma^2\left[L + \left(\frac{L-1/2}{L}\right)R\right]$$

$$E\left\{U^-\right\} = \frac{m^2}{2L} + 2\sigma^2 L = 2\sigma^2\left(L + \frac{R}{2L}\right)$$

(6-108)

and

$$\text{var}\left\{U^+\right\} = \frac{4}{N}\left[\sigma^4 L + \left(\frac{L-1/2}{L}\right)m^2\sigma^2 + \frac{m^4}{16L^2}\right]$$

$$= \frac{4}{N}\sigma^4\left[L + 2\left(\frac{L-1/2}{L}\right)R + \frac{R^2}{4L^2}\right]$$

(6-109)

$$\text{var}\left\{U^-\right\} = \frac{4}{N}\left(\sigma^4 L + \frac{m^2\sigma^2}{2L} + \frac{m^4}{16L^2}\right)$$

$$= \frac{4}{N}\sigma^4\left(L + \frac{R}{L} + \frac{R^2}{4L^2}\right)$$

Note that for $L = 1$ (the conventional SSME) and thus $L_\varepsilon = 0$, i.e., $\varepsilon = 1/2$, Eq. (6-108) agrees with Eq. (6-103) and Eq. (6-109) agrees with the combination of Eqs. (6-49) and (6-52). Furthermore, for sufficiently large L, the moments of $U^\pm$ given in Eqs. (6-108) and (6-109) reduce to

$$E\left\{U^+\right\} = 2\sigma^2\left(L + R\right), \quad E\left\{U^-\right\} = 2\sigma^2 L$$

(6-110)

$$\text{var}\left\{U^+\right\} = \frac{4}{N}\sigma^4\left(L + 2R\right), \quad \text{var}\left\{U^-\right\} = \frac{4}{N}\sigma^4 L$$

which correspond to those of the ideal (perfect symbol timing) SSME.

Finally, we note that for other values of ε between the best quantized ones, namely, $\varepsilon = L_\varepsilon/L$ which yield the same performance as the ideal SSME, and the worst quantized ones, namely, $\varepsilon = \left(L_\varepsilon + 1/2\right)/L$ which yield the most degradation in performance, the modified SSME will have a performance between these two extremes.

6.12 Other Modulations

Thus far, we have considered the behavior and performance of the SSME for the class of M-PSK ($M \geq 2$) modulations with and without frequency uncertainty. As we shall show in this section, it is also possible to use the same basic SSME structure (with perhaps slight modification) to provide SNR estimation for offset quadrature phase-shift keying (OQPSK) as well as non-constant envelope modulations such as QAM. As before, the performance of the estimator is still independent of the data symbol sequence as well as the carrier phase and allows for the same enhancement by increasing the number of pairs of observables per symbol in accordance with the true value of SNR.

6.12.1 Offset QPSK

For the case of M-PSK, we indicated in Section 6.1 that the kth transmitted complex symbol in the interval $(k-1)T \leq t \leq kT$ can be represented in the form $d_k = e^{j\phi_k}$, where ϕ_k takes on one of M phases uniformly spaced around the unit circle. A special case of the above, corresponding to $M = 4$, results in conventional quadrature phase-shift keying (QPSK). It is well-known that on nonlinear channels OQPSK provides a performance advantage since it reduces the maximum fluctuation in the signal amplitude by limiting the maximum phase change to 135 deg rather than 180 deg. Since for OQPSK the complex representation of a symbol extends over one and one-half symbols (because of the offset between the I and Q channels), it cannot conveniently be represented in the polar form $d_k = e^{j\phi_k}$ as above. Rather, one should consider the I and Q channel modulations separately. Thus, it is of interest to investigate whether the SSME can be easily modified to accommodate OQPSK and, if so, how its performance is affected. For convenience, we consider only the I&D implementation of the SSME since the same conclusions that will be reached also apply to the multiple samples per symbol version.

Corresponding to the kth QPSK symbol $d_k = e^{j\phi_k} = (a_k + jb_k)/\sqrt{2}$, where a_k and b_k are independent binary (± 1) symbols, the OQPSK transmitter sends $a_k/\sqrt{2}$ during the interval $(k-1)T \leq t \leq kT$ and $b_k/\sqrt{2}$ during the interval $(k-1/2)T \leq t \leq (k+1/2)T$. Thus, after complex demodulation by the receiver carrier with frequency uncertainty ω and unknown phase ϕ, the kth complex baseband received signal in the I channel is described by

$$y_I(t) = \frac{1}{\sqrt{2}}ma_k e^{j(\omega t + \phi)} + n_I(t), \quad (k-1)T \leq t \leq kT \qquad (6\text{-}111)$$

where as before $n_I(t)$ is a zero-mean AWGN process. The signal in Eq. (6-111) is, as before, input to first and second I-channel half-symbol I&Ds operating over

the intervals $(k-1)T \leq t \leq (k-1/2)T$ and $(k-1/2)T \leq t \leq kT$, respectively. Analogous to Eq. (6-14), the outputs of these I&Ds are given by

$$
\begin{aligned}
Y_{I_{\alpha k}} &= \frac{1}{\sqrt{2}} m a_k \frac{1}{T} \int_{(k-1)T}^{(k-1/2)T} e^{j(\omega t + \phi)} dt + \frac{1}{T} \int_{(k-1)T}^{(k-1/2)T} n_Q(t)\, dt \\
&= \left[m a_k / \left(2\sqrt{2} \right) \right] e^{j\phi} e^{j\omega(k-3/4)T}\, \text{sinc}\,(\delta/4) + n_{I_{\alpha k}}
\end{aligned}
\tag{6-112}
$$

$$
\begin{aligned}
Y_{I_{\beta k}} &= \left(\frac{1}{\sqrt{2}} m a_k \frac{1}{T} \int_{(k-1/2)T}^{kT} e^{j(\omega t + \phi)} dt + \frac{1}{T} \int_{(k-1/2)T}^{kT} n_I(t)\, dt \right) e^{-j\theta_k} \\
&= \left(\left[m a_k / \left(2\sqrt{2} \right) \right] e^{j\phi} e^{j\omega(k-3/4)T} e^{j\omega T/2}\, \text{sinc}\,(\delta/4) + n_{I_{\beta k}} \right) e^{-j\theta_k}
\end{aligned}
$$

where $n_{\alpha k}$ and $n_{\beta k}$ are complex Gaussian noise variables with zero mean and variance σ^2, and $e^{-j\theta_k}$ is a phase compensation that accounts for the possible adjustment of the kth second-half sample for phase variations across a given symbol due to the frequency offset.

Similarly, the kth complex baseband received signal in the Q channel is described by

$$
y_Q(t) = \frac{1}{\sqrt{2}} m b_k e^{j(\omega t + \phi)} + n_Q(t), \quad (k-1/2)T \leq t \leq (k+1/2)T
\tag{6-113}
$$

where $n_Q(t)$ is also a zero-mean AWGN process independent of $n_I(t)$. The signal in Eq. (6-113) is input to first and second Q-channel half-symbol I&Ds operating over the intervals $(k-1/2)T \leq t \leq kT$ and $kT \leq t \leq (k+3/2)T$, respectively. Analogous to Eq. (6-112), the outputs of these I&Ds are given by

$$
\begin{aligned}
Y_{Q_{\alpha k}} &= \frac{1}{\sqrt{2}} m b_k \frac{1}{T} \int_{(k-1/2)T}^{kT} e^{j(\omega t + \phi)} dt + \frac{1}{T} \int_{(k-1/2)T}^{kT} n_Q(t)\, dt \\
&= \left[m b_k / \left(2\sqrt{2} \right) \right] e^{j\phi} e^{j\omega(k-1/4)T}\, \text{sinc}\,(\delta/4) + n_{Q_{\alpha k}}
\end{aligned}
\tag{6-114}
$$

$$
\begin{aligned}
Y_{Q_{\beta k}} &= \left(\frac{1}{\sqrt{2}} m b_k \frac{1}{T} \int_{kT}^{(k+3/2)T} e^{j(\omega t + \phi)} dt + \frac{1}{T} \int_{kT}^{(k+3/2)T} n_Q(t)\, dt \right) e^{-j\theta_k} \\
&= \left(\left[m b_k / \left(2\sqrt{2} \right) \right] e^{j\phi} e^{j\omega(k-1/4)T} e^{j\omega T/2}\, \text{sinc}\,(\delta/4) + n_{Q_{\beta k}} \right) e^{-j\theta_k}
\end{aligned}
$$

Separately taking the half-symbol sums and differences of the Y_I's and Y_Q's results in the following:

$$
\begin{aligned}
u_{I_k}^{\pm} &= Y_{I_{\alpha k}} \pm Y_{I_{\beta k}} e^{-j\theta_k} \\
&= \left(\frac{ma_k}{2\sqrt{2}}\right) e^{j\phi} e^{j\omega(k-3/4)T} \operatorname{sinc}\left(\frac{\delta}{4}\right) \left[1 \pm e^{j([\delta/2]-\theta_k)}\right] + n_{I_{\alpha k}} \pm n_{I_{\beta k}} e^{-j\theta_k} \\
&\triangleq s_{I_k}^{\pm} + n_{I_k}^{\pm}
\end{aligned}
\tag{6-115}
$$

and

$$
\begin{aligned}
u_{Q_k}^{\pm} \\
&= Y_{Q_{\alpha k}} \pm Y_{Q_{\beta k}} e^{-j\theta_k} \\
&= \left(\frac{mb_k}{2\sqrt{2}}\right) e^{j\phi} e^{j\omega(k-1/4)T} \operatorname{sinc}\left(\frac{\delta}{4}\right) \left[1 \pm e^{j([\delta/2]-\theta_k)}\right] + n_{Q_{\alpha k}} \pm n_{Q_{\beta k}} e^{-j\theta_k} \\
&\triangleq s_{Q_k}^{\pm} + n_{Q_k}^{\pm}
\end{aligned}
\tag{6-116}
$$

Note by comparison of Eq. (6-112) with Eq. (6-114) that an additional phase shift of an amount $\omega T/2$ exists in the $u_Q^{\pm}$'s relative to the $u_I^{\pm}$'s, which would not be present if one were to generate the comparable I&D outputs for conventional QPSK. In principle, this phase shift could be perfectly compensated for if one had knowledge of the frequency uncertainty ω. However, in the absence of this exact knowledge, the best one could do at this point would be to multiply the $u_Q^{\pm}$'s by $e^{-j\hat{\omega}T/2}$, which ultimately would result in a degradation in performance if one were first to combine the $u_I^{\pm}$'s and $u_Q^{\pm}$'s into a complex quantity and then to proceed with the formation of the SSME in the same manner as for QPSK. Rather than compensate the phase shift at this point in the implementation, we proceed instead to separately form the averages of the squared norms of the $u_I^{\pm}$'s and $u_Q^{\pm}$'s over the N-symbol duration of the observation resulting in

$$
\begin{aligned}
U_I^{\pm} &= \frac{1}{N} \sum_{k=1}^{N} |u_{I_k}^{\pm}|^2 = \frac{1}{N} \sum_{k=1}^{N} \left[\left|s_{I_k}^{\pm}\right|^2 + \left|n_{I_k}^{\pm}\right|^2 + 2\operatorname{Re}\left\{s_{I_k}^{\pm}\left(n_{I_k}^{\pm}\right)^*\right\}\right] \\
U_Q^{\pm} &= \frac{1}{N} \sum_{k=1}^{N} |u_{I_k}^{\pm}|^2 = \frac{1}{N} \sum_{k=1}^{N} \left[\left|s_{Q_k}^{\pm}\right|^2 + \left|n_{Q_k}^{\pm}\right|^2 + 2\operatorname{Re}\left\{s_{Q_k}^{\pm}\left(n_{Q_k}^{\pm}\right)^*\right\}\right]
\end{aligned}
\tag{6-117}
$$

Since taking the magnitude of the $u_I^\pm$'s and the $u_Q^\pm$'s eliminates the relative phase shift between these quantities noted above, then it is straightforward to show that combining $U_I^\pm$ (delayed by $T/2$) with $U_Q^\pm$ results in a pair of signals $U^\pm$ that have the identical statistics as those for conventional QPSK. In particular, setting the half-symbol phase compensation $\theta_k = \omega_{sy}T/2$ (independent of k), then the signal term corresponding to the kth term in the average would be given by

$$\left|s_k^\pm\right|^2 = \left|s_{I_k}^\pm\right|^2 + \left|s_{Q_k}^\pm\right|^2 = m^2 \left(\frac{a_k^2 + b_k^2}{2}\right) \, \text{sinc}^2\left(\frac{\delta}{4}\right) \left[\frac{1 \pm \cos\left(\delta_{sy}/2\right)}{2}\right]$$

$$= m^2 \, \text{sinc}^2\left(\frac{\delta}{4}\right) \left[\frac{1 \pm \cos\left(\delta_{sy}/2\right)}{2}\right] \triangleq m^2 h^\pm \tag{6-118}$$

where as before $\delta_{sy} = \delta - \omega_{sy}T$.

To see how one can implement a universal SSME structure that will handle OQPSK as well as conventional QPSK, we proceed as follows. Consider partitioning the results of inputting the I- and Q-channel baseband signals to half-symbol I&Ds into even and odd outputs. That is, we define $Y_{I_{\alpha k}}$ and $Y_{Q_{\beta,k-1}}$, which correspond to half-symbol integrations in the interval $(k-1)T \leq t \leq (k-1/2)T$, as *odd* outputs, and $Y_{I_{\beta k}}$ and $Y_{Q_{\alpha k}}$, which correspond to half-symbol integrations in the interval $(k-1/2)T \leq t \leq kT$, as *even* outputs. Then, for conventional QPSK, since $u_{I_k}^\pm$ is formed from the sum and difference of $Y_{I_{\alpha k}}$ and $Y_{I_{\beta k}}$ and $u_{Q_k}^\pm$ is formed from the sum and difference of $Y_{Q_{\alpha k}}$ and $Y_{Q_{\beta,k-1}}$, we can say that $u_{I_k}^\pm$ is formed from the kth even and odd outputs, whereas $u_{Q_k}^\pm$ is formed from the kth even and $(k-1)$st (i.e., the preceding) odd outputs. On the other hand, since for OQPSK $u_{I_k}^\pm$ is still formed from the sum and difference of $Y_{I_{\alpha k}}$ and $Y_{I_{\beta k}}$ but $u_{Q_k}^\pm$ is formed from the sum and difference of $Y_{Q_{\alpha k}}$ and $Y_{Q_{\beta k}}$, we can say that both $u_{I_k}^\pm$ and $u_{Q_k}^\pm$ are formed from the kth even and odd outputs. Thus, from this viewpoint, the only difference in the SSME implementation between OQPSK and conventional QPSK is that for the former the Q-channel sum and difference signals are formed from the corresponding even and *succeeding* odd half-symbol I&D outputs, whereas for the latter the Q-channel sum and difference signals are formed from the *same* even but the *preceding* odd half-symbol I&D outputs. Other than this minor difference in implementation, the two SSMEs would yield performances identical to that given previously in this chapter.

6.12.2 QAM

For the case of QAM with an M-symbol square signal constellation, the kth transmitted complex symbol in the interval $(k-1)\,T \leq t \leq kT$ can be represented in the form $d_k = d_{Ik} + jd_{Qk}$ where d_{Ik} and d_{Qk} are independent, identically distributed (iid) RVs that take on the values $\pm 1, \pm 3, \cdots, \pm(\sqrt{M}-1)$ with equal probability. It is straightforward to show that the mean and variance of $U^\pm$ are, analogous to Eq. (6-8), given by

$$E\left\{U^\pm\right\} = 2\sigma^2 + E\left\{\left|s_k^\pm\right|^2\right\}$$

$$\mathrm{var}\left\{U^\pm\right\} = \frac{4}{N}\sigma^2\left(E\left\{\left|s_k^\pm\right|^2\right\} + \sigma^2\right)$$

(6-119)

where now $\left|s_k^\pm\right|^2 = m^2 h\left|d_k\right|^2$ and thus

$$E\left\{\left|s_k^\pm\right|^2\right\} = m^2 h E\left\{\left|d_k\right|^2\right\} = \frac{2}{3}\left(M-1\right)m^2 h \qquad \text{(6-120)}$$

However, since in the case of QAM the average SNR is given by

$$R = \frac{m^2}{2\sigma^2}$$

$$R = \frac{\frac{2}{3}(M-1)m^2}{2\sigma^2}$$

(6-121)

then combining Eq. (6-121) with Eq. (6-121) and substituting the result in Eq. (6-119), we obtain

$$E\left\{U^\pm\right\} = 2\sigma^2\left(1 + h^\pm R\right)$$

$$\mathrm{var}\left\{U^\pm\right\} = \frac{4}{N}\sigma^4\left(1 + 2h^\pm R\right)$$

(6-122)

which is identical with the second relations in Eq. (6-8). Thus, solving for R from Eq. (6-122) and following the same logic that led to the ad hoc SSME in Eq. (6-10), we conclude that no modification of this SSME is required to allow its use for estimating SNR when QAM is transmitted. Similarly, in view of the equivalence between Eqs. (6-122) and (6-8), we conclude that the performance is identical to that previously determined for M-PSK modulations.

6.13 The Time-Multiplexed SSME

In Section 6.6, we described a means for potentially improving the performance of the conventional SSME by increasing the number of subdivisions (observables) per symbol beyond two (but still an even number). In particular, we showed that the variance of the so-modified estimator tracks (with a fixed separation from it) the Cramer–Rao bound on the variance of an SNR estimator over the entire range of SNR values. Implicit in the derivation of the expression for the variance of the SNR estimator was the assumption that the even number of subdivisions was the same for all symbols in the observation from which the SNR estimator was formed, and as such an optimum value of the number of subdivisions, denoted by $2L$, was determined for a given true SNR region, the totality of which spans the entire positive real line. Moreover, it was shown that, if one ignores the requirement of having the number of subdivisions be an even integer and proceeds to minimize with respect to L the expression for the variance derived as mentioned above, an optimum value of L can be determined *for every value of true SNR*. The resulting estimator was referred to as the *fictitious* SSME and resulted in a lower bound on the performance of the practical realizable SSME corresponding to integer L.

In this section, we show how one can in practice turn the fictitious SNR estimator into a non-fictitious one. In particular, we demonstrate an implementation of the SSME that allows one to approach the unrestricted optimum value of L (to the extent that it can be computed as the average of a sum of integers) at every true SNR value. More specifically, the proposed approach, herein referred to as the *time-multiplexed SSME*, allows each symbol to possess its own number of subdivisions arranged in any way that, on the average (over all symbols in the observed sequence), achieves the desired optimum value of L. Furthermore, we propose an algorithm for *adaptively* achieving this optimum value of L when in fact one has no a priori information about the true value of SNR. Once again for simplicity of the discussion, we consider the case wherein the symbol pulse shape is assumed to be rectangular, and thus the observables from which the estimator is formed are the outputs of I&Ds.

A block diagram of the complex baseband time-multiplexed SSME is illustrated in Fig. 6-14 with the input signal in the kth interval $(k-1)T \leq t \leq kT$ as described by Eq. (6-13). Consider uniformly subdividing the kth symbol interval into $2L_k$ (L_k integer) subdivisions each of length $T_k/2 = (T/L_k)/2$. In each of these L_k pairs of split symbol intervals, we apply the signal in Eq. (6-9) to first and second half-symbol normalized (by the integration interval) I&Ds, the outputs of which are summed and differenced to form the signals $\left\{ u_{kl}^{\pm} \triangleq s_{kl}^{\pm} + n_{kl}^{\pm}, l = 1, \cdots, L_k \right\}$. For each k, the $u_{kl}^{\pm}$'s are iid; however, their statistics vary from symbol to symbol. Denote the relevant symbol-dependent
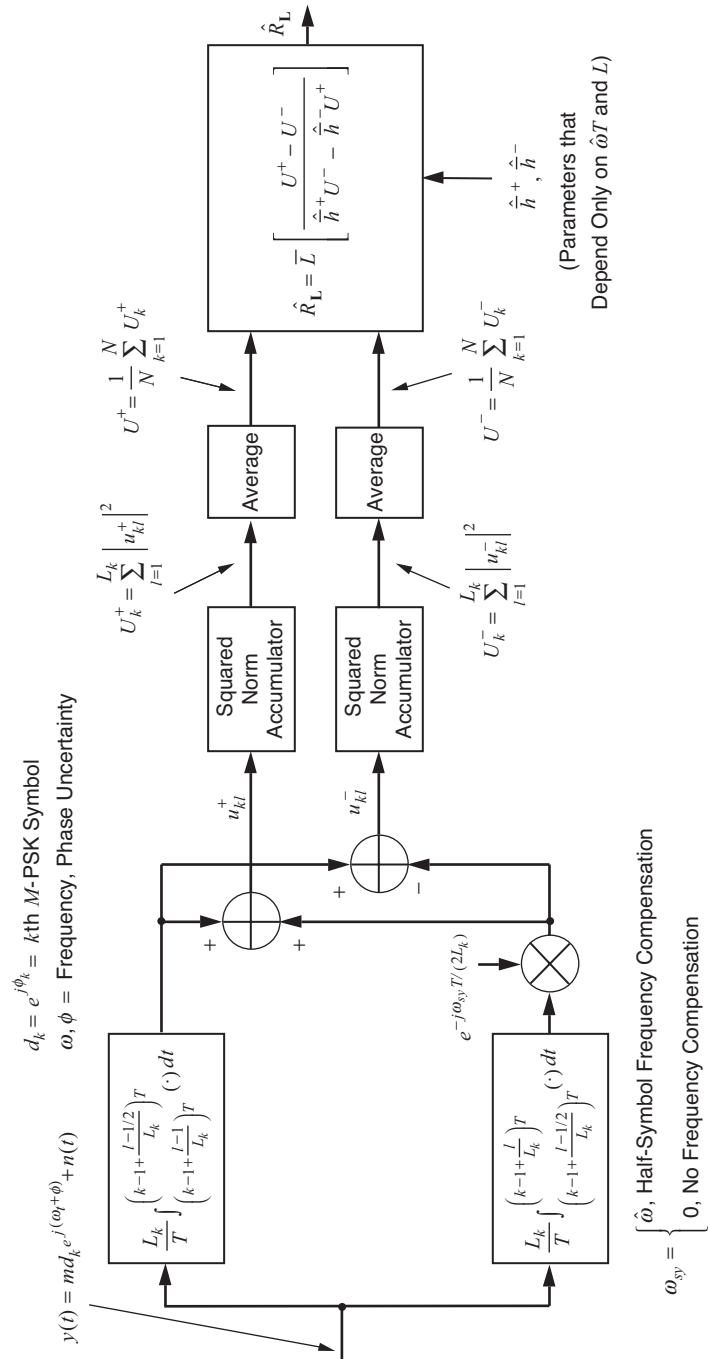
Fig. 6-14. Time-multiplexed split-symbol moments estimator of SNR for *M*-PSK modulation.

parameters of the signal and noise components of $u_{kl}^{\pm}$ as $m_k^2, \sigma_k^2, h_k^{\pm}$, and the SNR in the kth symbol as $R_k = m_k^2 / \left(2\sigma_k^2\right)$. In particular, $\sigma_k^2 = \sigma^2 L_k$ is the variance per component (real and imaginary) of $n_{kl}^{\pm}$, and the mean-squared value of $s_{kl}^{\pm}$ can be expressed as[6]

$$\left|s_{kl}^{\pm}\right|^2 = m_k^2 h_k^{\pm} \tag{6-123}$$

where, because of the normalization of the I&Ds, $m_k^2 = m^2$ independently of k, and $h_k^{\pm}$ is again a parameter that reflects the amount of frequency offset and the degree to which it is compensated for. Specifically,

$$h_k^{\pm} = \operatorname{sinc}^2\left(\frac{\delta_k}{4}\right) \frac{1 \pm \cos\left(\delta_{k_{sy}}/2\right)}{2} \tag{6-124}$$

where $\delta_k \triangleq \omega T_k, \delta_{k_{sy}} \triangleq \delta_k - \omega_{sy} T_k = (\omega - \omega_{sy}) T_k$, with ω_{sy} the compensation frequency applied to the second half-symbol I&D outputs.

Based on the above, each $\left|u_{kl}^{\pm}\right|^2 = \sigma_k^2 \chi_2^2\left(2h_k^{\pm} R_k\right)$, where $\chi_n^2(\mu)$ denotes a (generally non-central) chi-squared RV with n degrees of freedom, non-centrality parameter μ, and unit variances for each degree of freedom. In general, we know that $E\left\{\chi_n^2(\mu)\right\} = n + \mu$ and $\operatorname{var}\left\{\chi_n^2(\mu)\right\} = 2n + 4\mu$ for all n and μ. Furthermore, using [8, Eq. (2.39)] for the inverse moments of central chi-squared RVs, we have for even n and $\mu = 0$, $E\left\{[\chi_n^2(0)]^{-1}\right\} = (n-2)^{-1}$ and $E\left\{[\chi_n^2(0)]^{-2}\right\} = \left[(n-2)(n-4)\right]^{-1}$. Expressions for higher-order moments of $\chi_n^2(\mu)$ or its reciprocal can be determined using [8, Eq. (2.47)].

Now for each k define $U_k^{\pm} = \sum_{l=1}^{L_k} \left|u_{kl}^{\pm}\right|^2 / L_k$. Then, based on the above chi-squared characterization of $\left|u_{kl}^{\pm}\right|^2$, and recognizing that the true SNR to be estimated is given by

$$R = R_k L_k = \frac{m^2}{2\sigma^2} \tag{6-125}$$

we have $U_k^{\pm} = \left(\sigma_k^2/L_k\right)\chi_{2L_k}^2\left(2h_k^{\pm} R_k L_k\right) = \sigma^2 \chi_{2L_k}^2\left(2h_k^{\pm} R\right)$ with first mean and variance

$$E\left\{U_k^{\pm}\right\} = 2\sigma^2 \left(L_k + h_k^{\pm} R\right)$$

$$\operatorname{var}\left\{U_k^{\pm}\right\} = 4\sigma^4 \left(L_k + 2h_k^{\pm} R\right) \tag{6-126}$$

---

[6] Note that σ^2 is the variance per component of the $u_k^{\pm}$'s in the conventional SSME corresponding to $L = 1$ in each symbol interval.

Solving for R in terms of $E\{U_k^\pm\}$ from the first equation in Eq. (6-126), we obtain

$$R = L_k \left[\frac{E\{U_k^+\} - E\{U_k^-\}}{h_k^+ E\{U_k^-\} - h_k^- E\{U_k^+\}} \right] \tag{6-127}$$

At this point, we could proceed as we did in Section 6.1 by replacing expected values of $U_k^\pm$ with their sample values to obtain estimates of R from each symbol, and then averaging over the N estimates obtained from the N symbols, resulting in the ad hoc estimator

$$\hat{R}'_{\mathbf{L}} = \frac{1}{N} \sum_{k=1}^{N} L_k \left[\frac{U_k^+ - U_k^-}{h_k^+ U_k^- - h_k^- U_k^+} \right] \tag{6-128}$$

where $\mathbf{L} = (L_1, L_2, \cdots, L_N)$ denotes the oversampling vector for the N-symbol observation. Unfortunately, this has the potential of being a very bad estimator, because from our previous analyses we have observed that both the bias and the variance of the split-symbol estimate become unbounded if it is based on only a single symbol, i.e., $N = 1$. If $\{L_k\}$ takes on only a few discrete values, we could avoid this singularity by grouping symbols with the same L_k, obtaining an estimate from each group, and then averaging the estimates from all the groups. A better approach is to first average the $U_k^\pm$'s prior to forming them into an ad hoc estimator. Specifically, we form $U^\pm = (1/N) \sum_{k=1}^{N} U_k^\pm$, which has the chi-squared characterization $U^\pm = (\sigma^2/N)\chi^2_{2\bar{L}N}(2\bar{h}^\pm NR)$, where $\bar{L} = (1/N) \sum_{k=1}^{N} L_k$ and $\bar{h}^\pm = (1/N) \sum_{k=1}^{N} h_k^\pm$. The mean and variance of $U^\pm$ are immediately given by

$$E\{U^\pm\} = 2\sigma^2 \left(\bar{L} + \bar{h}^\pm R \right)$$

$$\text{var}\{U^\pm\} = \left(4\sigma^4/N \right) \left(\bar{L} + 2\bar{h}^\pm R \right) \tag{6-129}$$

Solving for R in terms of $E\{U^\pm\}$, we obtain

$$R = \bar{L} \left[\frac{E\{U^+\} - E\{U^-\}}{\bar{h}^+ E\{U^-\} - \bar{h}^- E\{U^+\}} \right] \tag{6-130}$$

Now we replace expected values with sample values and $\bar{h}^\pm$ with estimates $\hat{\bar{h}}^\pm$ based on an estimate $\hat{\omega}$ of the frequency offset ω in this single equation to get our SNR estimate:

$$\hat{R}_{\mathbf{L}} = \bar{L} \left[\frac{U^+ - U^-}{\hat{\bar{h}}^+ U^- - \hat{\bar{h}}^- U^+} \right] \qquad (6\text{-}131)$$

The equations defining both the estimator $\hat{R}_{\mathbf{L}}$ and the underlying observables $U^{\pm}$ in terms of standard chi-squared random variables are identical in form to those obtained for the special case of uniform subsampling of all the symbols, $\mathbf{L} = (L, L, \cdots, L)$. The parameters $\bar{L}$, $\bar{h}^{\pm}$ for the general case reduce to the constants L, $h^{\pm}$ for the special case. The special case $\mathbf{L} = (L, L, \cdots, L)$ produces the estimator $\hat{R}_L$ of Section 6.6, where we assumed constant L for all symbols. Thus, we can apply our previous performance calculations for $\text{var}\{\hat{R}_L\}$ to obtain the corresponding expressions for $\text{var}\{\hat{R}_{\mathbf{L}}\}$ by simply replacing L and $h^{\pm}$ in those expressions with $\bar{L}$ and $\bar{h}^{\pm}$, respectively. In the case of zero frequency offset, we now can achieve the variance expression for any value of $\bar{L}$ achievable by *averaging* integers, not just integer values of L themselves. For large N, this means that we can achieve the performance of our fictitious estimator $\hat{R}_{\bullet}$ for a very dense set of values of R satisfying $L_{\bullet}(R) = R/\sqrt{2} \geq 1$. Of course, the fictitious estimator remains fictitious for $L_{\bullet}(R) = R/\sqrt{2} < 1$ (i.e., the region of R where we did not attempt to use it as a benchmark).

6.13.1 An Adaptive SSME

Given that $\hat{R}_{\mathbf{L}}$ achieves the performance of $\hat{R}_{\bar{L}}$, we now have a method for adaptively selecting the oversampling factor L. We can start with an initial guess, and then increase or decrease L in response to intermediate SNR estimates $\hat{R}_{\mathbf{L}}$ based on the symbols observed up to now. The key point is that the estimator $\hat{R}_{\mathbf{L}}$ at any point in time achieves exactly the same performance as the estimator $\hat{R}_L$ with $L = \bar{L}$, based on the same cumulative number of symbols. Thus, no symbols are wasted if an adaptive SNR estimation algorithm starts out with a non-optimum value of L but adapts over time to generate a vector sequence $\mathbf{L}$ for which the average $\bar{L}$ approaches the optimum value of L, namely, $L = L_{\bullet}(R) = R/\sqrt{2}$. Figure 6-15 is a flow diagram of such an adaptive scheme modeled after the robust version of the generalized SSME discussed in Section 6.7, wherein the integer values of L are restricted to the set $b^l, l = 0, 1, 2, 3, \cdots$ for some integer base b. The operation of the scheme is described as follows.

Initially, consider an observation of n symbols and set $L_k = L = 1, k = 1, 2, \cdots, n$. Next, evaluate the sum and difference accumulated variables $U^{\pm}$ for the n symbol observation. Proceed to evaluate the SNR estimator $\hat{R} = \hat{R}_{\mathbf{L}}(U^{\pm})$ in accordance with Eq. (6-131) taking note of the fact that, for this choice of $\mathbf{L}$, $\bar{L} = 1$. Next, we compare the current value of L, namely $L = 1$, to the
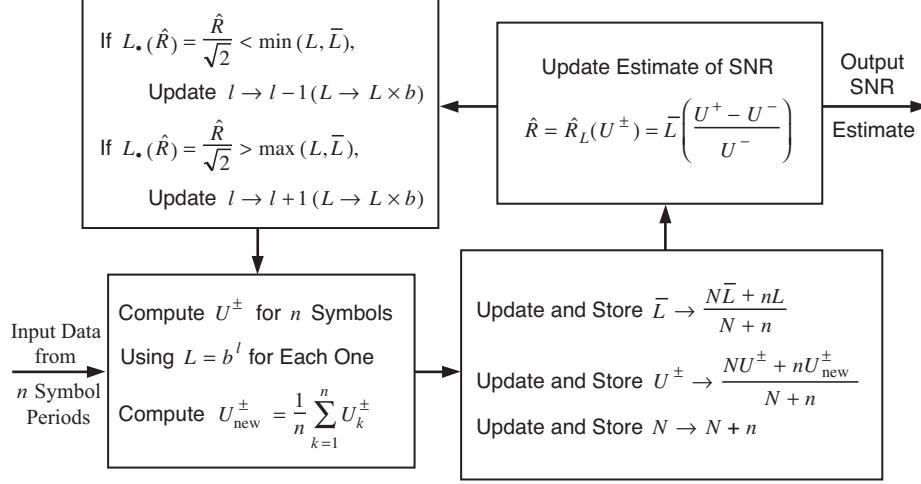
Fig. 6-15. A robust adaptive SSME scheme.

desired optimum value of L, based however on the current estimate of R, i.e., $L_\bullet(\hat{R}) = \hat{R}/\sqrt{2}$, to get an indication of how close we are to where we are headed. If $L_\bullet(\hat{R})$ exceeds unity, which on the average is likely to be the case if the true SNR is greater than $\sqrt{2}$, increment L by multiplying it by b and proceed to process the next n input symbols, as will be described momentarily. On the other hand, if $L_\bullet(\hat{R})$ is less than or equal to unity, which on the average is likely to be the case if the true SNR is less than or equal to $\sqrt{2}$, then leave L unchanged[7] and again proceed to process the next n input symbols. Moving on to the next set of n symbols, compute new values of $U^\pm$, denoted by $U^\pm_{\text{new}}$, using the updated value of L as determined above for all $L_k, k = n+1, n+2, \cdots 2n$. Let N denote the running average of the number of symbols. (Assume that initially N was set equal to n corresponding to the first set of observed symbols.) Update the current values of $U^\pm$ with the new $U^\pm_{\text{new}}$ values according to the weighted average $\left(NU^\pm + nU^\pm_{\text{new}}\right)/(N + n)$ and store these as $U^\pm$. Update the running average of L in accordance with $\left(N\bar{L} + nL\right)/(N + n)$ and store this as $\bar{L}$. Finally, update the value of N to $N+n$ and store this new value. Using the updated $U^\pm$, compute an updated SNR estimate $\hat{R} = \hat{R}_{\mathbf{L}}\left(U^\pm\right)$ in accordance with Eq. (6-131). Next, using this updated SNR estimate, compute the updated estimate of the optimum L, namely, $L_\bullet(\hat{R}) = \hat{R}/\sqrt{2}$ and use it to update the current value of L in accordance with the following rule:

---

[7] As we shall see shortly, in all other circumstances of this nature, we would proceed to decrement L by dividing it by b. However, since the current value of L is already equal to unity, which is the smallest nonzero integer, we cannot reduce it any further.

$$\text{If } L_\bullet\left(\hat{R}\right) < \min\left(L, \bar{L}\right), \text{ then divide } L \text{ by } b$$

$$\text{If } L_\bullet\left(\hat{R}\right) > \max\left(L, \bar{L}\right), \text{ then multiply } L \text{ by } b \qquad (6\text{-}132)$$

$$\text{If } \min\left(L, \bar{L}\right) \le L_\bullet\left(\hat{R}\right) \le \max\left(L, \bar{L}\right), \text{ do not change } L$$

Finally, using the updated value of L, proceed to process the next n symbols, whereupon the algorithm repeats as described above.

To illustrate the behavior of the robust adaptive SSME scheme, simulations were conducted to demonstrate the rate at which $\bar{L}$ converges to the true optimum L and also the manner in which this convergence takes place. The first simulation, illustrated in Fig. 6-16, demonstrates the ideal performance of the scheme assuming no frequency error, i.e., $\hat{\bar{h}}^+ = 1, \hat{\bar{h}}^- = 0$, and the following parameters: $R = 10, b = 2, n = 10$. By "ideal" is meant that the same adaptive feedback rule for updating L as in Eq. (6-132) is used except that a magic genie is assumed to be available to provide the true SNR, R, to the update rule rather than using the estimate of R. That is, the update of L in accordance with Eq. (6-132) is carried out using $L_\bullet(R)$ rather than $L_\bullet(\hat{R})$. The horizontal axis in Fig. 6-16 is measured in discrete units of time corresponding to the cumulative number of n-symbol batches processed each with a fixed value of L. The vertical axis represents two different indicators of the performance corresponding to the behavior of $\log_2 L$ and $\log_2 \bar{L}$ as they are updated in each cycle through the feedback loop. For the assumed parameters, the optimum value of L to which the scheme should adapt is given in logarithmic terms by $\log_2 L_\bullet(10) = \log_2\left(10/\sqrt{2}\right) = 2.822$. From the plots in Fig. 6-16, we observe that $\log_2 L$ quickly rises (in three steps) from its initial value of $\log_2 1 = 0$ to $\log_2 8 = 3$ and then eventually fluctuates between $\log_2 8 = 3$ and $\log_2 4 = 2$ with a 3:1 or 4:1 duty cycle. At the same time, $\log_2 \bar{L}$ smoothly rises toward the optimum $\log_2 \bar{L}_\bullet$, converging asymptotically to this limit (with indistinguishable difference) in fewer than 20 cycles of the feedback loop or, equivalently, 200 symbol intervals.

Figure 6-17 is an illustration of the actual performance of the scheme as illustrated in Fig. 6-15, i.e., in the absence of a magic genie to provide the true SNR. The same parameter values as in Fig. 6-16 were assumed, and 10 different trials were conducted. Also superimposed on this figure for the purpose of comparison is the $\log_2 \bar{L}$ magic genie performance obtained from Fig. 6-16. For 6 out of the 10 trials, the actual performance was indistinguishable from that corresponding to the magic genie. For the remaining 4 trials, $\log_2 \bar{L}$ overshoots its target optimum value but still settles toward this value within 20 cycles of the algorithm. For all 10 trials, there is a small dispersion from the optimum level even after 40 cycles. This is due to residual error in estimating R after $N = 400$ symbols since the variance only decreases as $1/N$.
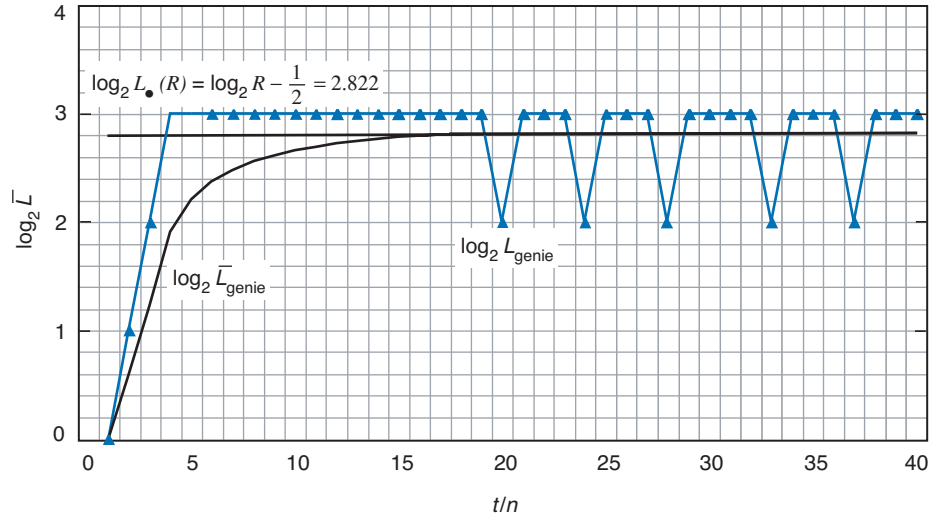
Fig. 6-16. Ideal performance of the robust adaptive SSME scheme. (Adaptive SSME with magic genie estimate of true SNR, $R = 10$.)
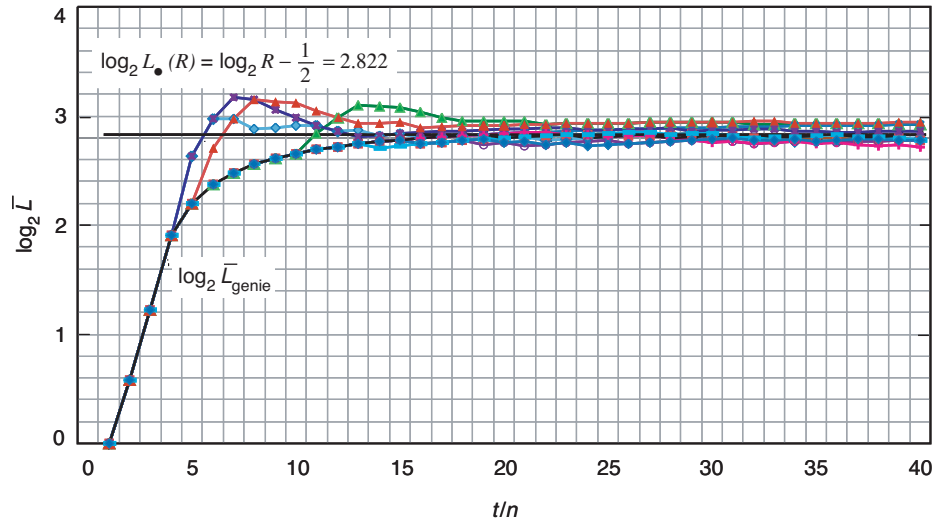

Fig. 6-17. Actual performance of the robust adaptive SSME scheme. (Adaptive SSME: 10 trials with $N = 400$, $n = 10$, true $R = 10$.)

References

[1] D. R. Pauluzzi and N. C. Beaulieu, "A Comparison of SNR Estimation Techniques for the AWGN Channel," *IEEE Trans. Commun.*, vol. 48, pp. 1681–1691, October 2000.

[2] M. K. Simon and A. Mileant, "SNR Estimation for the Baseband Assembly," *The Telecommunications and Data Acquisition Progress Report 42-85, January–March 1986*, Jet Propulsion Laboratory, Pasadena, California, pp. 118–126, May 15, 1986. http://ipnpr.jpl.nasa.gov/

[3] B. Shah and S. Hinedi, "The Split Symbol Moments SNR Estimator in Narrow-Band Channels," *IEEE Trans. Aerosp. Electron. Syst.*, vol. AES-26, pp. 737–747, September 1990.

[4] S. Dolinar, "Exact Closed-Form Expressions for the Performance of the Split-Symbol Moments Estimator of Signal-to-Noise Ratio," *The Telecommunications and Data Acquisition Progress Report 42-100, October–December 1989*, Jet Propulsion Laboratory, Pasadena, California, pp. 174–179, February 15, 1990. http://ipnpr.jpl.nasa.gov/

[5] Y. Feria, "A Complex Symbol Signal-to-Noise Ratio Estimator and its Performance," *The Telecommunications and Data Acquisition Progress Report 42-116, October–December 1993*, Jet Propulsion Laboratory, Pasadena, California, pp. 232–245, February 15, 1994. http://ipnpr.jpl.nasa.gov/

[6] M. K. Simon and S. Dolinar, "Signal-to-Noise Ratio Estimation for Autonomous Receiver Operation," *GLOBECOM 2004 Conference Record*, Dallas, Texas, November 2004.

[7] M. Simon and S. Dolinar, "Improving Signal-to-Noise Ratio Estimation for Autonomous Receivers," *The Interplanetary Network Progress Report*, vol. 42-159, Jet Propulsion Laboratory, Pasadena, California, pp. 1–19, November 15, 2004. http://ipnpr.jpl.nasa.gov/

[8] M. K. Simon, *Probability Distributions Involving Gaussian Random Variables: A Handbook for Engineers and Scientists*, Norwell, Massachusetts: Kluwer Academic Publishers, 2002.

[9] M. Abramowitz and I. A. Stegun, *Handbook of Mathematical Functions with Formulas, Graphs, and Mathematical Tables*, 9th ed., New York: Dover Press, 1972.

[10] A. Papoulis, *Probability, Random Variables, and Stochastic Processes*, New York: McGraw-Hill, 1965.

[11] H. L. V. Trees, *Detection, Estimation, and Modulation Theory*, vol. 1, New York: Wiley, 1968.

[12] C. M. Thomas, *Maximum Likelihood Estimation of Signal-to-Noise Ratio*, Ph.D. thesis, University of Southern California, Los Angeles, 1967.

[13] S. J. Dolinar, "Cramer-Rao Bounds for Signal-to-Noise Ratio and Combiner Weight Estimation," *The Telecommunications and Data Acquisition Progress Report 42-86, April–June 1986*, Jet Propulsion Laboratory, Pasadena, California, pp. 124–130, August 15, 1986. http://ipnpr.jpl.nasa.gov/

Appendix 6-A
Derivation of Asymptotic Mean and Variance of SSME

In this appendix, we derive the asymptotic expressions for the mean and variance of the SSME as given by Eqs. (6-32) and (6-33), respectively. For convenience, we repeat the expressions for the mean and variance of $U^\pm$, namely,

$$E\left\{U^\pm\right\} = 2\sigma^2 + \left|s_k^\pm\right|^2 = 2\sigma^2\left(1 + h^\pm R\right)$$

$$\text{var}\left\{U^\pm\right\} = \frac{4}{N}\sigma^2\left(\left|s_k^\pm\right|^2 + \sigma^2\right) = \frac{4}{N}\sigma^4\left(1 + 2h^\pm R\right)$$

(A-1)

Starting from the definition of $g\left(U^+, U^-\right)$ in Eq. (6-10), we evaluate its first and second partial derivatives as

$$\frac{\partial g}{\partial U^\pm} = \frac{\pm\left(\hat{h}^+ - \hat{h}^-\right)U^\mp}{\left(\hat{h}^+U^- - \hat{h}^-U^+\right)^2}$$

$$\frac{1}{2}\frac{\partial^2 g}{\partial\left(U^\pm\right)^2} = \frac{\left(\hat{h}^+ - \hat{h}^-\right)\hat{h}^\mp U^\mp}{\left(\hat{h}^+U^- - \hat{h}^-U^+\right)^3}$$

(A-2)

The quantity $\hat{h}^+U^- - \hat{h}^-U^+$ that appears in the denominator of $g\left(U^+, U^-\right)$ and its partial derivatives is evaluated at the point $\left(U^+, U^-\right) = \left(E\{U^+\}, E\{U^-\}\right)$ as

$$\hat{h}^+ E\left\{U^-\right\} - \hat{h}^- E\left\{U^+\right\} = 2\sigma^2\left[\left(\hat{h}^+ - \hat{h}^-\right) + \left(\hat{h}^+h^- - \hat{h}^-h^+\right)R\right] \quad \text{(A-3)}$$

The second term in parentheses in Eq. (A-3) evaluates to zero for cases 0, 2a, 2b, and 2c for which the frequency estimate is perfect, i.e., $\hat{\omega} = \omega$, since in this instance $\hat{h}^\pm = h^\pm$. The numerators of $g\left(U^+, U^-\right)$ and its partial derivatives evaluated at the point $\left(U^+, U^-\right) = \left(E\left\{U^+\right\}, E\left\{U^-\right\}\right)$ are, respectively,

$$E\left\{U^{+}\right\} - E\left\{U^{-}\right\} = 2\sigma^2\left(h^{+} - h^{-}\right)R$$

$$\pm\left(\hat{h}^{+} - \hat{h}^{-}\right)E\left\{U^{\mp}\right\} = \pm\left(\hat{h}^{+} - \hat{h}^{-}\right)2\sigma^2\left(1 + h^{\mp}R\right) \tag{A-4}$$

$$\left(\hat{h}^{+} - \hat{h}^{-}\right)h^{\mp}E\left\{U^{\mp}\right\} = \left(\hat{h}^{+} - \hat{h}^{-}\right)h^{\mp}2\sigma^2\left(1 + h^{\mp}R\right)$$

Substituting the expressions in Eqs. (A-3) and (A-4) into Eqs. (6-10) and (A-2), we obtain

$$g\big|_{(E\{U^{+}\},E\{U^{-}\})} = \frac{\left(h^{+} - h^{-}\right)R}{\hat{h}^{+} - \hat{h}^{-} + \left(\hat{h}^{+}h^{-} - \hat{h}^{-}h^{+}\right)R}$$

$$\frac{\partial g}{\partial U^{\pm}}\bigg|_{(E\{U^{+}\},E\{U^{-}\})} = \pm\frac{1}{2\sigma^2}\frac{\left(\hat{h}^{+} - \hat{h}^{-}\right)\left(1 + h^{\mp}R\right)}{\left[\hat{h}^{+} - \hat{h}^{-} + \left(\hat{h}^{+}h^{-} - \hat{h}^{-}h^{+}\right)R\right]^2} \tag{A-5}$$

$$\frac{1}{2}\frac{\partial^2 g}{\partial\left(U^{\pm}\right)^2}\bigg|_{(E\{U^{+}\},E\{U^{-}\})} = \frac{1}{4\sigma^4}\frac{\left(\hat{h}^{+} - \hat{h}^{-}\right)h^{\mp}\left(1 + h^{\mp}R\right)}{\left[\hat{h}^{+} - \hat{h}^{-} + \left(\hat{h}^{+}h^{-} - \hat{h}^{-}h^{+}\right)R\right]^3}$$

Finally, substituting the expression for $\text{var}\left\{U^{\pm}\right\}$ in Eq. (A-1) along with the expressions in Eq. (A-5) into Eq. (6-31) results after some simplification in

$$E\left\{\hat{R}\right\} = \frac{\left(h^{+} - h^{-}\right)R}{\hat{h}^{+} - \hat{h}^{-} + \left(\hat{h}^{+}h^{-} - \hat{h}^{-}h^{+}\right)R}$$

$$+ \frac{1}{N}\frac{\left(\hat{h}^{+} - \hat{h}^{-}\right)\left(\hat{h}^{+} + \hat{h}^{-}\right)}{\left[\hat{h}^{+} - \hat{h}^{-} + \left(\hat{h}^{+}h^{-} - \hat{h}^{-}h^{+}\right)R\right]^3}$$

$$\times\left\{1 + \left(h^{+} + h^{-} + \frac{\hat{h}^{+}h^{-} + \hat{h}^{-}h^{+}}{\hat{h}^{+} + \hat{h}^{-}}\right)R + 2h^{+}h^{-}R^2\right\} + O\left(\frac{1}{N^2}\right)$$

$$\tag{A-6}$$

and

$$\text{var}\left\{\hat{R}\right\} =$$

$$\frac{1}{N} \frac{\left(\hat{h}^{+} - \hat{h}^{-}\right)^{2}}{\left[\hat{h}^{+} - \hat{h}^{-} + \left(\hat{h}^{+}h^{-} - \hat{h}^{-}h^{+}\right)R\right]^{4}}$$

$$\times \left\{2 + 4\left(h^{+} + h^{-}\right)R + \left[\left(h^{+} + h^{-}\right)^{2} + 6h^{+}h^{-}\right]R^{2} + 4h^{+}h^{-}\left(h^{+} + h^{-}\right)R^{3}\right\}$$

$$+ O\left(\frac{1}{N^{2}}\right) \tag{A-7}$$

which are repeated as Eqs. (6-32) and (6-33) in Section 6.4.2.